GOING WITH THE FLOW:
SELECTIVE PHOSPHODIESTERASE 4D7 (PDE4D7) REGULATION OF VASCULAR ENDOTHELIAL CELL RESPONSES TO FLUID SHEAR STRESS

by

Jonah Burke-Kleinman

A thesis submitted to the Department of Biomedical and Molecular Sciences

In conformity with the requirements for

the degree of Master of Science

Queen's University

Kingston, Ontario, Canada

August, 2018

Abstract

Vascular endothelial cells (VECs) regulate their phenotype in response to the frictional force exerted by the flowing blood, fluid shear stress (FSS). The hemodynamics dictating this force determine, to a large extent, the likelihood that a given region of a blood vessel will develop atherosclerotic plaque. In linear arterial segments, VECs are exposed to high laminar unidirectional FSS (15-20 dyne/cm^2), whereas in bifurcations, arches and branch points, VECs encounter low magnitude/oscillating or otherwise disturbed FSS (0-4 dyne/cm^2). High laminar FSS promotes establishment of an adaptive VEC phenotype, characterized by the expression of anti-thrombotic, anti-inflammatory and anti-atherogenic genes. Conversely, low and oscillating flow causes VECs to express pro-inflammatory, pro-thrombotic genes and adopt an athero-prone phenotype. Previous studies have identified mechanosensory signalling molecules that allow VECs to sense and respond to FSS, which include vascular endothelial cadherin (VE-cadherin), platelet endothelial cell adhesion molecule 1 (PECAM-1) and vascular endothelial growth factor receptor 2 (VEGFR2). Research conducted by our group has previously shown that exchange protein activated by cAMP (EPAC1) and cyclic nucleotide phosphodiesterase 4D (PDE4D) populate a multi-protein signalling complex along with VE-cadherin. These proteins function together to regulate VEC barrier function, cell morphology and gene expression of in response to FSS. Now, we have investigated this compartmentalized signalling complex in greater detail, and have identified that one splice variant, namely phosphodiesterase 4D7 (PDE4D7), controls VEC gene regulation in response to FSS, while another, PDE4D5, does not. Indeed, we show that PDE4D7 silencing with siRNA attenuates the upregulation of krüppel-like factor 2 (*KLF2*), endothelial nitric oxide synthase (*eNOS*) and thrombomodulin (*TM*) in VECs exposed to FSS. This work identifies a potential novel specific therapeutic target for the treatment or prevention of atherosclerosis and improves our understanding of mechanosensory signal transduction in the vascular endothelium.

Lay Abstract

Heart disease is the most common cause of all death in the world. In heart disease, arteries which carry the blood become blocked by the buildup of fats and debris. The cells that form the insides of arteries depend on the flowing blood to keep them healthy. In places where the blood flow is fast, the cells protect against heart disease. However, in places where the blood flow is slow or disturbed, like eddies in a riverbend, the cells are more likely to allow heart disease to occur. Our research looks at how cells from arteries behave under different types of blood flow. By figuring out how these cells adjust their behaviour to the flowing blood, we can try to develop drugs to treat or prevent heart disease. We have discovered that one particular protein, “PDE4D7”, controls how the cells sense the flowing blood and adjust their behaviour.

Co-Authorship

All the experiments presented in this thesis were conceptualized by Jonah Burke-Kleinman and Dr. Donald Maurice, and conducted by Jonah Burke-Kleinman.

Acknowledgements

There are numerous people that made this work possible, and deserve thanks.

To my friends and family: thank you for supporting me throughout my time at Queen’s.

To the Queen’s Sailing Team: thank you for making my time here more fun than I possibly could have imagined, and giving me one of the most rewarding experiences of my life.

To Jodi, Paulina, and Ariana, the Maurice Lab students: thank you for your continual support. It was a daily pleasure being surrounded by such brilliant and hard-working colleagues. To Jodi MacKeil: thank you for patiently training me as a 4^{th}-year student, and introducing me to several important assays.

To Bibi: your role to myself and others is way more than that of a typical lab technician. Thank you for infecting us with your positivity and energy – traits you possess at superhuman levels.

To Dr. Donald Maurice: thank you for welcoming me into your laboratory, and for being an excellent supervisor throughout the process. I learned more from our collective conversations than I thought possible.

To my partner Katie: thank you for your companionship and acceptance of a scientist’s lifestyle. You are my constant in a world of variables.

Thank you to the CIHR for providing the funding to make this research possible.

Table of Contents

List of Figures

List of Tables

List of Abbreviations

AJ	Adherens junction
AKAP	A-kinase anchoring protein
cAMP	Cyclic adenosine monophosphate
CDC42	Cell division control protein 42 homolog
cGMP	Cyclic guanosine monophosphate
DAPI	4’,6’-diamidino-2-phenylindole dihydrochloride hydrate
DNA	Deoxyribonucleic acid
ECM	Extracellular matrix
eNOS	Endothelial nitric oxide synthase
EPAC1	Exchange protein activated by cAMP
ERK	Extracellular signal-regulated kinase
FSS	Fluid shear stress
GPCR	G-protein coupled receptor
HAEC	Human aortic endothelial cell
hTERT	Human telomerase reverse transcriptase
ICAM-1	Intercellular adhesion molecule 1
IκB-α	Inhibitor of kappa-light-chain-enhancer of activated B-cells alpha
KLF2	Krüppel-like factor 2
MAPK	Mitogen-activated protein kinase
NF-κB	Nuclear factor kappa-light-chain-enhancer of activated B-cells
PAK	p21-activated kinase
PDE	Cyclic nucleotide phosphodiesterase
PDE4D7	Phosphodiesterase gene family 4, gene D, splice variant 7
PECAM-1	Platelet endothelial cell adhesion molecule 1
RNA	Ribonucleic acid
RT-qPCR	Realtime quantitative polymerase chain reaction
siRNA	Short interfering RNA
TeloHAEC	Telomerase-immortalized human aortic endothelial cell
TM	Thrombomodulin
UCR1/2	Upstream conserved region 1/2
VCAM-1	Vascular cell adhesion molecule 1
VEC	Vascular endothelial cell
VEGFR2	Vascular endothelial growth factor receptor 2
VSMC	Vascular smooth muscle cell

Chapter 1

Introduction

For many years, vascular endothelial cells (VECs) were considered to be little more than a container for the blood – a contiguous monolayer of relatively inert cells in the shape of a tube through which the blood could flow. However, upon closer inspection, it has become abundantly evident that VECs actively fulfil a myriad of critical roles in blood vessel homeostasis including the regulation of vascular tone, permeability, inflammation, lipid metabolism, angiogenesis, and coagulation. Indeed, it is now largely recognized that VECs are very dynamic cells, able to switch phenotype between quiescent and activated states in response to their environment. Now, VECs are widely regarded as key players in the initiation and progression of cardiovascular diseases such as atherosclerosis. We choose to study these cells because even incremental advances in this field could have large impacts on the massive global burden of heart disease, which is responsible for ~30% of mortality worldwide[1].

In the presence of circulating risk factors for atherosclerosis such as lipids and immune cells, one could be forgiven for expecting atherosclerotic plaques to develop everywhere in the vasculature equally. In fact, we find that this is not the case – rather, there are specific sites in the vasculature where we frequently find plaques, and other places where there are rarely any. The cause of this phenomenon appears to be haemodynamic in nature: the blood, as it flows, exerts a frictional force on the walls of the vessel termed fluid shear stress (FSS). In linear portions of large arteries, VECs are exposed to high magnitude unidirectional laminar FSS (15-30 dyne/cm^2)[2]. In regions such as bifurcations, arches or curvatures, VECs are subjected to low magnitude FSS (0-4 dyne/cm^2) oscillating between positive and negative velocity vectors[3]. These distinct hemodynamic force profiles impart major phenotypic changes in the endothelium. VECs exposed to high laminar FSS adopt an athero-protective phenotype and express anti-inflammatory, anti-thrombotic mediators. In marked contrast, VECs exposed to low or oscillating FSS adopt an athero-prone phenotype and upregulate the expression pro-inflammatory and pro-thrombotic genes. Indeed, it is in regions of low or oscillating FSS that atherosclerotic plaques form most preferentially[4]. By understanding the process by which this occurs, and how these kinetic forces are transduced into biochemical signals, we can identify therapeutic targets to prevent atherosclerotic plaque development initiation or progression.

There are a number of known mechanosensory proteins that allow VECs to sense and response to FSS. These include vascular endothelial cadherin (VE-cadherin), platelet endothelial cell adhesion molecule 1 (PECAM-1) and vascular endothelial growth factor receptor 2 (VEGFR2), which form a multimolecular complex at adherens junctions (AJs) and senses FSS as tension between cells[5]. While this is currently the most well-studied mechanosensors in VECs, others including the glycocalyx, integrins, ion channels and heterotrimeric G-protein coupled receptors (GPCRs) are also important.

Previous work by our lab identified a multiprotein complex involving VE-cadherin and other important signalling proteins: exchange protein activated by cyclic AMP (EPAC1) and cyclic nucleotide phosphodiesterase 4D (PDE4D)[6-8]. In this work, it was reported that PDE4D binds with EPAC1 and VE-cadherin at AJs in a complex that allows VECs to respond adaptively to FSS by aligning and elongating in the direction of flow, enhancing barrier function, and upregulating atheroprotective genes such as endothelial nitric oxide synthase (*eNOS*), krüppel-like factor 2 (*KLF2*) and thrombomodulin (*TM*). Other members of this putative complex include the small GTPase Rap1 along with VEGFR2 and PECAM-1. Through siRNA-mediated knockdown of EPAC1, Rap1 or

PDE4D, it was elucidated that each of these players are important regulators of the adaptive response to FSS. It was also found that PDE4D functions as a tether for EPAC1 and VE-cadherin in this signalling complex.

In an extension of this previous work, we were interested in discerning which of the numerous splice variants of PDE4D were responsible for maintaining this complex. In previous immunoprecipitation experiments with VE-cadherin, PDE4Ds consistent with the size of PDE4D5 / PDE4D7 were detected. To address questions of PDE4D(7) catalytic function vs. tethering function, and elucidate its role in the signalling complex further, we sought to create immortalized endothelial cell lines expressing a catalytically-dead PDE4D7, in addition to using siRNA-mediated knockdown of PDE4D5 and PDE4D7.

Now, we show that of the splice variants of PDE4D, PDE4D7 in particular occupies this signalling complex and controls VEC response to FSS. Upon siRNA knockdown of PDE4D7 specifically, but not PDE4D5, VECs alignment and elongation to FSS is impaired, as is the upregulation of atheroprotective genes. Advancing our knowledge of FSS mechanosensory signalling may be translatable to more than just the vascular endothelium, but in other shear-exposed organs such as the heart or the lymphatic system. Developing therapies targeting a single splice variant rather than all PDE4D would be valuable, as current pan-PDE4(D)-targeted treatments are limited by severe emetic effects[9]. By further understanding mechanisms of VEC function, alleviating cardiovascular diseases by targeting therapies to these functions becomes more possible.

Chapter 2

Literature Review

2.1 Emergence, structure and functionality of complex circulatory systems

As multi-cellular organisms grew larger, and surface-area to volume ratio decreased, it became more difficult for all the cells to receive adequate oxygen. Enter circulatory systems, which evolved as a means to overcome limits of oxygen diffusion from the environment. In addition to such primary roles as oxygen and nutrient delivery, the human cardiovascular system functions to mediate inflammatory responses, safeguard against and repair injury through hemostasis and angiogenesis. Specialized cells optimize flow dynamics and barrier function, as well as immune and coagulation factors. However, for all the functions that it has evolved to optimize, there are evolutionary trade-offs: a closed vascular system is necessarily branched and curved, creating micro-domains of flow disturbance vulnerable to dysfunction[10]. Furthermore, the human vascular system evolved to maximize fitness in an earlier era, and has not adapted to relatively recent changes in longevity, activity, and diet. Taken together, these principles form the basis for understanding cardiovascular disease today.

Structurally, larger arterial vessels are composed of three discrete layers: the *tunica adventitia*, the *tunica media* and the *tunica intima* (fig. 1). The adventitia is chiefly an innervated structural layer, rich in fibroblasts and collagen-containing extracellular matrix that provides the elastic and strength characteristics that allow the vessel wall to function during changes in blood flow and pressure. In addition, the layer can itself be vascularized by the *vaso vasorum*, small vascular structures that feed medial layer smooth muscle cells and facilitate the transit of resident macrophages, dendritic cells, as well as B- and T- lymphocytes between vascular and non-vascular spaces[11]. The adventitial layer may even assist in vessel repair, as it contains a progenitor cell niche for vascular smooth muscle cell (VSMC) and endothelial cell replenishment[12].

The internal and external elastic laminae border the tunica media, and contain small structural fenestrations to allow macromolecule diffusion. These laminae are composed primarily of type I and II collagen and elastin[13]. The tunica media of healthy blood vessels contains primarily vascular smooth muscle cells (VSMCs). Medial VSMCs function to adjust the lumen diameter through constriction and relaxation, controlling blood pressure and diverting blood flow. In response to various stimuli, including vascular injury, VSMCs can modulate their phenotype along a continuum bracketed by "contractile" and "synthetic" states. As their names imply, contractility is the dominant response of contractile VSMCs to changes in blood flow, while synthetic VSMCs are proliferative, migratory and can synthesize and deposit extracellular matrix (ECM) proteins. These cells play a large role in the progression of atherosclerosis or vascular restenosis. VSMCs rely closely on stimuli from the endothelial cells to control their state of contractility and phenotype.

The innermost layer, the tunica intima, is composed of vascular endothelial cells (VECs). These form a contiguous monolayer which serves as both dynamic border and an interface for the entirety of the body's blood. VECs are fine-tuned to respond to a multitude of circulating signals, and are responsible for regulating vascular tone, permeability, inflammation, lipid metabolism, angiogenesis, and coagulation[14]. These cells are dynamic, able to adopt multiple distinct phenotypes depending on the environment. In healthy blood vessels, VECs adopt a quiescent phenotype, maintain the barrier separating vascular and non-vascular spaces, and express anti-inflammatory, anti-thrombotic and vasodilatory proteins. Activated VECs, the phenotype adopted by cells exposed to situations such as wound healing, hypoxia and inflammation, are hyperpermeable, pro-inflammatory, pro-thrombotic and vasoconstrictive[15]. While these behaviours are adaptive and represent appropriate responses to injury or invasion by a foreign body, they can become mal-adaptive when engaged chronically. When circulating factors such as reactive oxygen species or oxidized low-density lipoproteins are elevated, or in patients with hypertension, hyperglycaemia, or hypercholesterolemia, endothelial cells can become chronically activated. The function of VECs is therefore central to vascular homeostasis and cardiovascular diseases[16].

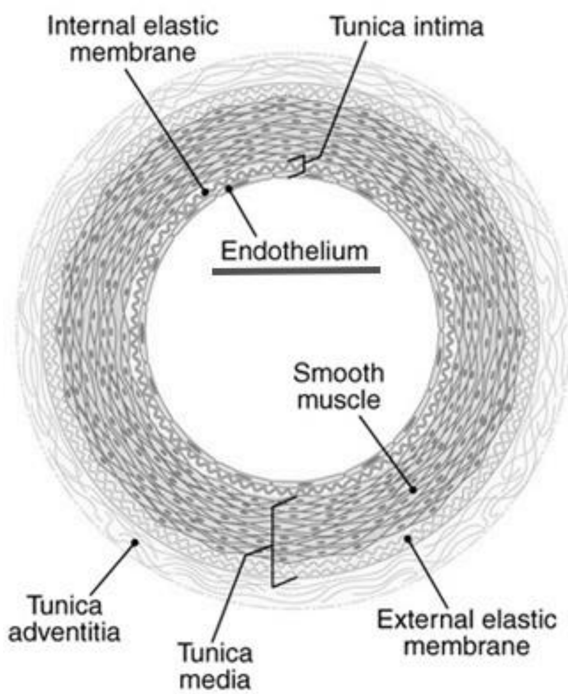

Figure 1. Artery cross-section.

Endothelial cells form the inner lining of large blood vessels. Image modified from dental histology prep course at ice.uthscsa.edu (http://ice.uthscsa.edu/dentalhistologyprepcourse/10%20tubular_organs/tubular_organs_print.html)

2.2 Fluid Shear Stress

In addition to circulating factors, there is another critical regulator of VEC phenotype and function. The flowing blood itself imparts a frictional force upon the endothelium, termed fluid shear stress (FSS). Fluid moving across a boundary will cause shear stress, the force vector for which is parallel to the vessel cross section. During development, FSS mediates development of the adult-like vascular tree, as well as the differentiation of arterial and venous structures[17]. Proper regulation of vascular tone and overall homeostasis is dependent upon the ability of VECs to sense and respond to FSS. Chronic alterations in blood flow can cause VEC-mediated remodelling to return FSS to a physiological set-point[18]. When FSS is chronically low, VECs promote constrictive vascular remodelling to increase blood flow and reset FSS to a favourable range.

Levels of FSS in the adult vascular system can be calculated by multiplying rate of flow by blood viscosity, and have been determined using various imaging techniques such as magnetic resonance[19], ultrasound[20] and computed tomography[21]. These calculations assume blood is a Newtonian fluid, which it is not, but are the reasonable approximation. In linear arterial segments, FSS levels range from 15-50 dyne/cm[22]. In non-linear vascular segments, including bifurcations and curvatures, FSS can be below 4 dyne/cm[23]. Generation of both forward and reverse flow velocities can occur at these points as well. High laminar unidirectional FSS promotes a healthy quiescent VEC phenotype, which take on a characteristically elongated morphology[24]. Low, oscillatory, or disturbed FSS predisposes VECs to developing activated and dysfunctional phenotypes that chronically are mal-adaptive.

Indeed, at these low FSS locations specifically are where the majority of atherosclerotic plaques and lesions are found. For instance, the infrarenal abdominal aorta, a site which correlates strongly with atherosclerotic plaque development, experiences flow reversal during diastole due to its large curvature[21]. The coronary arteries have FSS levels determined not only by systole and diastole but by the contractions of the heart muscle itself, which can disturb flow dynamics: dynamic compression of the coronary tunneled septal branches results in disturbed blood flow in the left anterior descending (LAD) artery[23]. Coronary calcifications are most frequently located here, in proximity of the septal branch origin. Because of this, and the fact that blockages of the LAD artery are so severe, it has become colloquially known as “the widowmaker artery”. In the thoracic aorta, lateral and proximal sites prone to atherosclerosis contain structural peculiarities which can cause disruption from laminar flow[25]. The carotid sinus in the internal carotid artery is another site predisposed to the development of atherosclerosis because of local hemodynamics[26] (fig. 2). Plaque progression and rupture, which can result in total vascular blockage, are particularly harmful in the coronary and carotid arteries, as it can lead to myocardial infarction or stroke respectively. Since it has been well established that FSS is a critical factor in determining the formation and location of atherosclerosis, investigating the mechanisms by which the VECs sense and respond to this force is imperative in understanding this disease and in developing therapeutic strategies to rectify or attenuate it.

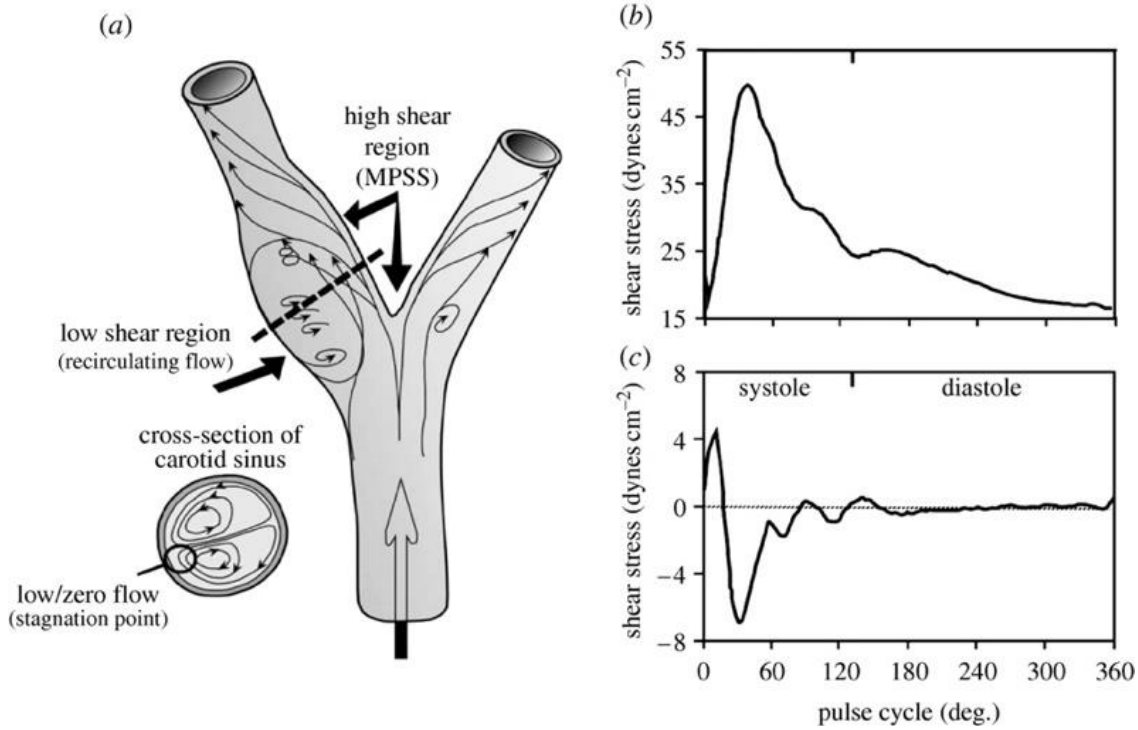

Figure 2. Fluid shear stress in the carotid artery.

Distinct profiles of FSS exist in adjacent locations in the vasculature. Image modified from [27]

2.3 Mechanosensors

So far, several molecules and pathways have been discovered that allow VECs to sense FSS, and can be found either on the luminal cellular membrane, in regions of cell-cell contacts called adherens junctions (AJs), or on the basal cellular membrane that interacts with the extracellular matrix (ECM). The process of mechanotransduction can be defined as the conversion of kinetic signals to biochemical signals. These numerous mechanosensory molecules have been found to sense FSS either as tension between cells[28] or as deflection, physical bending or structural deformation. Under laminar FSS, deflection is proportional to the product of shear force and sensor length, but under oscillatory shear, the velocity at the tips of those elements is $\pi/2$ out of phase with the shear force[29]. FSS-responsive elements include G-protein coupled receptors (GPCRs), surface glycoproteins, ion channels, integrins, platelet endothelial cell adhesion molecule 1 (PECAM-1), vascular endothelial cadherin (VE-cadherin), and the plasma membrane itself (fig. 3). After FSS onset, plasma membrane fluidity increases and activates heterotrimeric G proteins, with or without upstream GPCR activation[30]. This also activates transmembrane proteins such as the bradykinin receptor and the inward rectifying K+ ion channel. Previous work by our lab has focused on a mechanosensory complex involving VE-cadherin and other proteins[6], upon which we will elaborate.

The endothelial cell glycocalyx is attached to the plasma membrane, and contains glycoproteins involved in coagulation, hemostasis and fibrinolysis. It acts as a mechanosensor by forming a complex gel between the cell wall and the flowing blood, and linking with plasma proteins and lipids. Included are immunoglobulins such as intercellular adhesion molecule 1 (ICAM-1) and vascular cell adhesion molecule 1 (VCAM-1), ligands for integrins on leukocytes and platelets.

Glypican, one of two families of heparin sulfate proteoglycans, participates in direct mechanotransduction by activation endothelial nitric oxide synthase (eNOS) at caveolin-rich sites[31]. Syndecan-1, a member of the other family of heparin sulfate proteoglycans, interacts with the cytoskeleton, and transmits force from the luminal surface of the cell to distal locations such as adhesion or growth factor receptors[32]. In the absence of syndecan-1, VECs do not characteristically align or elongate in response to FSS[33].

Primary cilia located on the plasma membrane are microtubule-based structures, which protrude into the luminal space and change shape in response to FSS[34]. This increases intracellular Ca^{2+} and promotes downstream NO synthesis and vasodilation. Primary cilia can be present in static culture, but are lost when VECs are exposed to high levels of FSS *in vitro*[35]. Furthermore, *in vivo*, cilia have only been detected in VECs exposed to low FSS such as at arterial bifurcations. The presence of primary cilia reduces the expression of many VEC inflammatory genes such as *IL-1*, *IL-6*, *TNF-α*, *TGF-β*, *VCAM-1* and *E-selectin*[34]. In pulmonary VECs, application of FSS or stimulation with inflammatory cytokines TNF-α, IL-1β, and interferon-γ led to elongation of cilia[36]. Interestingly, primary cilia of VECs from pulmonary arterial hypertension (PAH) patients lengthened in response to FSS but not proinflammatory cytokines. The complete mechanisms underlying cilia signalling are not yet fully known.

The VEC cytoskeleton is also responsible for FSS mechanotransduction. Upon exposure to laminar FSS, cytoskeletal arrangements are apparent within minutes. Rho GTPases such as cell division control protein 42 homolog (Cdc42), Rho and Rac mediate this rearrangement[37]. Onset of FSS rapidly activates integrin αvβ3, inducing the transient inactivation of Rho, necessary for cytoskeletal adaptation to flow[38]. Morphological changes in VECs exposed to FSS have themselves been linked to signalling alterations. When forced to align by culturing VECs in micro-patterned lanes, classical FSS-induced transcription factor Krüppel-like factor 2 (*KLF2*) was upregulated in an actin-dependent manner[39]. When VECs were allowed to align to flow and re-oriented perpendicular to the FSS vector, inflammatory signalling pathways were activated such as nuclear factor kappa light chain enhancer of activated B cells (NF-κB). Alignment of VECs in the direction of FSS is therefore essential to the protective phenotype.

Integrins play a central role in VEC mechanotransduction and signal in response to FSS depending on the composition of the extracellular matrix (ECM) to which they bind. Integrin α2β1 is activated on collagen, but not fibronectin, whereas α5β1 and αvβ3 are activated on fibronectin and not collagen[40]. Fibronectin becomes the predominant ECM protein in early atherogenesis, so it is unsurprising that α5β1 and αvβ3 integrins contribute to inflammatory signalling. Downstream of fibronectin-dependent integrin activation, FSS activates p21-activated kinase (PAK), which can activate NF-κB and increase expression of ICAM-1 and VCAM-1[41]. Consistently, PAK is not activated on collagen. Integrin expression and matrix composition go hand-in-hand to modulate transduction of FSS-encoded signals.

There is evidence that certain G-protein coupled receptors (GPCRs) are important mechanosensors for FSS. Mechanical perturbations of the plasma membrane can lead to ligand-independent conformation changes in GPCRs; stimulation of VECs with FSS leads to increased bradykinin B_2 GPCR activation as measured by GPCR conformation-sensitive FRET[42]. Recently, it was discovered that GPR68 is a flow-sensitive GPCR required for FSS responses[43].

A high-throughput screen identified GPR68 as a critical transducer of FSS signals by measured changes in intracellular Ca^{2+} concentration in HeLa cells and HEK293T cells. Although these are not typically FSS-exposed cells, its relevance was confirmed when experiments in GPR68-deficient mice showed that flow-mediated artery dilation was impaired. Interestingly, GPR68 also functions as a pH sensitive GPCR[44].

One critically important VEC mechanosensory complex, and perhaps the most well studied thus far, involves VE-cadherin, PECAM-1 and vascular endothelial growth factor receptor 2 (VEGFR2) . In this junctional complex, PECAM-1 transmits mechanical force directly with VE-cadherin functioning as an adaptor, to activate VEGFR2 in a ligand-independent manner, activating phosphatidyloinositol-3-OH[45]. VE-cadherin also provides adhesive strength at adherens junctions, and is itself under tension.

PECAM-1 regulates intercellular adhesion and leukocyte transmigration by localizing to cell-cell borders in confluent VEC monolayers[46]. Application of FSS to cells in culture increases tension through PECAM-1 through enhanced association with vimentin, while tension through VE-cadherin decreases. Tension-mediated conformation change promotes phosphorylation of immune-receptor tyrosine-based inhibitory motifs (ITIMs) on the short intercellular domain of PECAM-1 by Src family kinases such as Fyn[47]. Phosphorylation of PECAM-1 occurs as a direct result of mechanical force from FSS, and not from any other upstream signalling events. Once phosphorylated, PECAM-1 recruits SHP-2, an SH2-domain-containing tyrosine phosphatase, which activated numerous downstream pathways including ERK1/2 and *eNOS*. Also induced by PECAM-1 phosphorylation are PI3K signalling and Akt/PKB activation, resulting in transient increases in NF-κB, as well as VEC alignment and elongation. Cells lacking PECAM-1 do not activate Src in response to FSS. *In vivo*, PECAM-1 knockout mice do not activate NF-κB and downstream inflammatory genes in regions of disturbed flow[48]. This pathway is therefore implicated in the earliest events of atherogenesis.

VE-cadherin is critical in transducing signals downstream of PECAM-1 – in its absence, PI3K/Akt signalling, integrin activation and VEC alignment and elongation in response to FSS to do not occur[45]. The extracellular domain of VE-cadherin forms homotypic Ca^{2+}-dependent interactions with neighbouring cells' VE-cadherin proteins. Intracellularly, it interacts with alpha- and beta- catenins, linking it to the cytoskeleton. It provides adhesive force between cells, but also senses tension, which decreases across VE-cadherin as FSS increases. Live imaging with a VE-cadherin FRET tension sensor construct in zebrafish revealed that loss of calcium signalling rapidly increases tension, suggesting a critical connection between those two pathways[49]. VE-cadherin is required for the upregulation of expression of numerous VEC-specific genes with roles in vascular stabilization, doing so by inhibiting polycomb activity on the gene promoters[50]. Predominantly, VE-cadherin acts as an adaptor for PECAM-1 and VEGFR2.

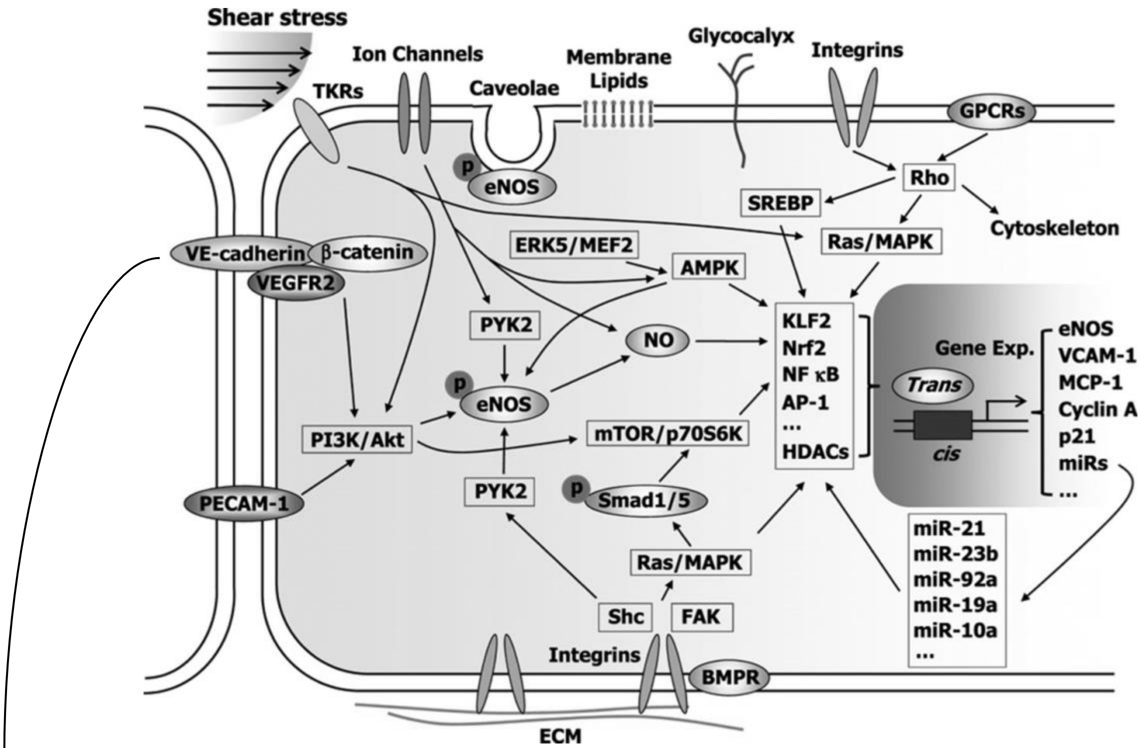

Figure 3A. Mechanotransduction signalling pathways.

VE-cadherin-based complex activates PI3K/Akt pathways to activate eNOS and upregulate KLF2. Modified from [51]

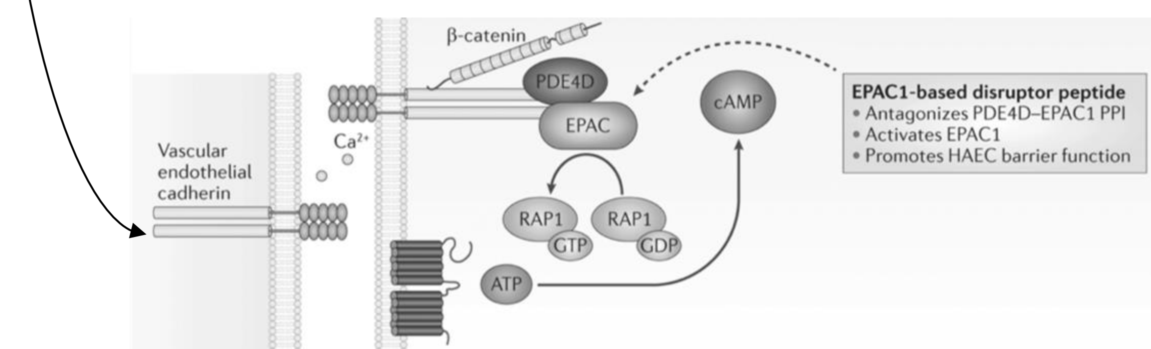

Figure 3B. VE-cadherin, EPAC1 and PDE4D complex

PDE4D, EPAC1 form a multiprotein complex with VE-cadherin, activating Rap1. Modified from [9].

2.4 FSS-mediated VEC phenotypic modulation

The signalling pathways activated by the above-described mechanosensors have important effects on the expression of many genes in VECs that impact phenotype. Certain genes are activated quickly and transiently by FSS, and others more slowly but chronically. These early / transiently activated genes are mostly angiogenic or pro-inflammatory, and include c-myc, activator protein-1 (AP-1), T cell factor (TCF), and NF-κB[52]. However, in disturbed flow, the continual stimulation of mechanosensors activates these otherwise transient genes in a sustained manner[53]. Under laminar FSS, a different subset of pathways remains induced, and largely promote the expression of anti-inflammatory, anti-thrombotic and anti-oxidative genes.

Perhaps the single most important transcription factor for adaptive response to FSS is kruppel-like factor 2, also known as lung Krüppel-like factor (KLF2/LKLF). It is a zinc-finger DNA-binding transcription factor responsible for inducing the expression of over 15% of FSS-dependent genes, and ~50% of genes highly regulated by FSS, including *eNOS*[54]. In VECs, KLF2 is upregulated only under laminar FSS, and not oscillatory FSS[4]. Both high laminar and pulsatile flow upregulate KLF2 and its paralog KLF4 in a sustained manner. In humans, *KLF2* expression is lowered at the outer wall of the bifurcation of the aorta and the iliac arteries, and at the branch of the common carotid artery from the aortic arch, where flow is disturbed[55]. Upregulation of KLF2 begins with activation of extracellular signal-regulated kinase 5 (ERK5), and proceeds through the induction of transcription factor myocyte enhancing factor 2 (MEF2)[2]. MEF2 binds to the MEF2 binding site located within the *KLF2* promoter and induces its expression. In addition, PI3K-dependent transcriptional coactivators p300/cAMP-responsive element binding protein (CBP), heterogenous ribonucleoprotein D (hnRNPD) and nucleolin also bind the *KLF2* promoter to regulate its expression. Post-transcriptional regulation of *KLF2* by microRNAs has also been reported. One such microRNA, miR-92a, binds the 3'-UTR of the *KLF2* mRNA, silencing its translation. Laminar FSS downregulates this miR-92a[56]. KLF2 also promotes the activation of antioxidant transcription factor Nrf2[57]. Both *KLF2* and Nrf2 reduce VEC inflammatory responses[58].

Of the genes regulated by KLF2, one of the most important in blood vessel homeostasis is *eNOS/NOS3*[59]. KLF2 and its coactivators p300/CBP bind the *eNOS* promoter region, causing long-term enhancement of *eNOS* expression. FSS increases PI3K activation and phosphorylation of Akt at Ser473[40], and Akt phosphorylates eNOS at Ser1177, activating the enzyme. Along with its cofactor tetrahydrobiopterin (BH_4), activated eNOS produces nitric oxide (NO) from L-arginine. The NO synthesized by *eNOS* in VECs diffuses to the underlying VSMCs, where it activates soluble guanylate cyclase increasing cGMP, lowering Ca^{2+} and allowing muscle relaxation. In addition to promoting vasodilation, NO regulates cell proliferation, leukocyte adhesion, ROS, and platelet aggregation[60]. Therefore, eNOS is essential to healthy blood vessel homeostasis. Interestingly, KLF2 has also been shown to inhibit the activation of several vasoconstrictive pathways such as endothelin-1 and angiotensin converting enzyme (ACE), so its regulation of vascular tone extends beyond just eNOS.

Another important gene regulated by KLF2 is thrombomodulin (*TM*), an anti-thrombotic regulator. TM is an integral membrane glycoprotein present on VECs, where it sequesters thrombin, a serine/threonine protease, and restricts its interaction with circulating procoagulant substrates such as fibrinogen[61]. This interaction also enhances the affinity of TM for protein C

(PC), increasing its activation 1000-fold relative to the unbound form. TM-bound thrombin cleaves PC to created activated protein (APC), which inactivates factor Va and VIIIa by proteolysis – a potent anti-coagulatory function. APC can also impair myocyte cytokine production, and circulating thrombin itself can induce VEC pro-inflammatory signalling by NF-κB activation and downstream IL-6, IL-8, E-selectin and MCP-1 signalling. KLF2 binds the TM promoter and positively regulates its expression in VECs exposed to laminar FSS.

While transcription factors like KLF2 are upregulated by atheroprotective flow, others like NF-κB can be activated by disturbed flow. NF-κB acts as a transcription factor for various inflammatory, immune and developmental related genes including adhesion molecules such as ICAM-1, VCAM-1 and E-selectin[62]. In cultured VECs, low or disturbed FSS activates NF-κB in a sustained manner – conversely, high laminar FSS activates NF-κB rapidly but transiently[63]. Inactive NF-κB is retained in the cytosol by IκB inhibitor proteins, which are phosphorylated by IκB kinase (IKK), ubiquitinated and degraded, thereby allowing NF-κB to translocate to the nucleus and promote the expression of target genes. Activation of IKK and subsequent degradation of IκB are induced by FSS[64]. This process is regulated in concert with the surrounding microenvironment, as NF-κB is activated by FSS only on fibronectin, but not collagen or laminin[65]. FSS also increases histone H3 acetylation, permitting transcription factors such as NF-κB, CREB and AP-1 to access FSS response genes.

The coordination of VEC responses to FSS relies on crosstalk between these critical transcription factors, KLF2 and NF-κB. Each one inhibits the transcriptional activity of the other; NF-κB reduces KLF2 expression by inhibiting MEF2 through regulation of HDAC4/5[66]. Conversely, KLF2 and KLF4 inhibit NF-κB function and adhesion molecule expression. KLF2 competes with NF-κB for binding of CBP/p300, a coactivator required for maximum NF-κB activity[59]. *KLF2* also inhibits nuclear activity of ATF2, a component of heterodimeric transcription factor AP-1, in response to laminar FSS. Therefore, VEC phenotype can be viewed as a product of competition between master transcription factors *KLF2* and NF-κB. When environmental factors combine to tip the scales towards NF-κB, VECs become atheroprone.

Onset of shear stress triggers the induction of ion channels, Src-family and VEGFR2 tyrosine kinases, extracellular signal-regulated kinases (ERKs), c-Jun amino-terminal kinases (JNKs), p38 mitogen-activated protein kinase and AKT serine/threonine kinases, PECAM-1 ITIM kinases, as well as NF-κB. VE-cadherin is implicated in flow-induced NF-κB activation. Under laminar shear, VECs adapt to the flow and these events are gradually downregulated, but under oscillatory / disturbed flow these pathways are activated in a sustained manner[1].

Increases in blood flow and FSS result in the release of vasodilators such as nitric oxide (NO), prostacyclin PGI_2, and endothelial-derived hyperpolarizing factor (EDHF)[67]. Conversely, decreases in FSS and blood flow can promote the release of endothelin-1, a vasoconstricting agent[68]. Laminar shear stress suppresses cell cycle progression by upregulating cyclin-dependent kinase inhibitor 1 (p21) and reducing phosphorylation of retinoblastoma protein (Rb)[69]. Conversely, low / disturbed flow enhances apoptosis and proliferation of VECs. These are but a few examples of factors modulated by VECs in response to different levels of FSS. In order to maintain optimal vascular tone, VECs must have specific mechanotransduction machinery to convert physical stimuli into biochemical signals.

2.5 Cyclic adenosine monophosphate signalling

The ubiquitous second messenger molecule cyclic 3'-5' adenosine monophosphate (cAMP) regulates a multitude of cellular processes[70]. It is synthesized by a large group of transmembrane adenylyl cyclases (ADCY1-9), and one cytosolic soluble adenylyl cyclase (ADCY10). Transmembrane ADCYs are turned on when agonists activate the $G\alpha_s$-coupled GPCRs. Cyclic AMP diffuses in the cell and activates downstream effectors such as protein kinase A (PKA) or exchange protein activated by cAMP (EPAC), cAMP-activated ion channels and Popeye domain-containing proteins (Popdcs). In addition to its synthesis, cAMP levels are also regulated by their hydrolysis by a group of enzymes called cyclic nucleotide phosphodiesterases (PDEs) [71]. PDEs hydrolytically cleave cAMP into 5' AMP, a metabolite which does not significantly regulate cAMP effectors listed above. Cyclic AMP signalling regulates a range of processes including cell adhesion, migration, proliferation, inflammation and barrier function.

The first class of cAMP effector identified were the PKAs: a group of tetrameric holoenzymes that, when inactive, consist of two regulatory domains and two catalytic domains. Mammalian cells can express several of the four PKA-R subunits, RI or RII. Upon binding of cAMP, to sites within these regulatory domains, the inhibited catalytic subunits are released from this inhibition and are then free to phosphorylate a multitude of downstream targets. PKA is one of the most-researched kinases, in part due to its unique tetrameric architecture, and in part due to its involvement in a tremendous number of signalling processes across all cell types. Although some have reported that PKA activity is involved in allowing VECs to respond to changes in FSS[72], our laboratory's findings do not support this contention[6].

The other major cAMP-signalling effector class of proteins are the exchange proteins activated by cAMP (EPACs). EPACs are guanine nucleotide exchange factors for members of the Ras superfamily including Rap1, Rap2 and R-Ras. There are two isoforms (EPAC1 and EPAC2) differentially expressed between cell types: EPAC1 is expressed throughout the body, including in VECs, whereas EPAC2 is mostly found in cells derived from the brain, kidney and pancreas. In the basal cAMP-free state, EPAC exists in an auto-inhibitory conformation with the N-terminal region on top of the C-terminal region, blocking the active site. Upon cAMP binding, the regulatory lobe moves away to expose to catalytic site, also revealing a lipid binding motif targeting EPAC to the plasma membrane. The cAMP effectors PKA and EPAC are capable of either functioning independently, converging synergistically, or opposing each other in regulating specific cellular functions.

Another effector class for cAMP regulated proteins are the Popeye domain containing proteins (POPDCs). These are expressed in multiple cell types and tissues, present in multiple subcellular compartments, and bind cAMP with high affinity. Perhaps the most studied of these is blood vessel epicardial substance (Bves), also known as Popdc1. Bves controls cell shape and movement by signalling through Rac1 / Cdc42[73], although their roles in communicating changes in FSS to VECs remains unclear.

Cyclic AMP also regulates the activity of certain ion channels, known as cyclic nucleotide-gated (CNG) channels. These were discovered in the context of light-sensitive rod cell channels being activated by cGMP in 1985[74]. Channels in rod and cone cells discriminate between cAMP and cGMP ligands, whereas others such as those found in olfactory sensory neurons respond equally well to both. CNGA1 and CNGA2 channels are both expressed in VECs across different species[75]. In human cerebral microvascular endothelial cells, cAMP activates CNG channels to induce Ca^{2+} influx and increased gap junction coupling[76]. The roles of CNG channels in VEC transduction of FSS signals is largely unexplored, but likely involved in crosstalk with cAMP and calcium signaling pathways.

Initially, the idea that cAMP signalling was compartmentalized was met with considerable resistance. With the discovery of A-kinase anchoring proteins (AKAPs), a mechanism of subcellular tethering of cAMP effectors become clear. Different AKAPs are capable of serving multiple roles including tethering PKA to subcellular locations, tethering substrates to promote selective phosphorylation, scaffolding signalosomes with different proportions of PKAs, ADCYs, phosphatases (which dephosphorylate proteins), EPACs and PDEs. By restricting cAMP signalling into spatially and/or temporally by generating distinct compartments, these systems have evolved to become highly specific for certain cellular processes.

2.6 Cyclic nucleotide phosphodiesterases

As introduced above, the two cyclic nucleotide second messengers cAMP and GMP are degraded by cyclic nucleotide phosphodiesterases (PDEs), which catalyze the hydrolysis of their phosphodiester bond. Twenty-one mammalian genes encode 11 unique gene families by virtue of sequence homology. These 11 unique mammalian PDE genes families, are capable of producing over 100 distinct isozymes through alternative mRNA splicing and transcriptional processing. While structurally related, PDEs differ in cellular function, subcellular localization, affinities for cAMP and cGMP, catalytic / kinetic properties and responses to certain activators, inhibitors and effectors. Although some functional redundancy likely exists, evidence suggests that most PDE variants play unique roles in the cell.

PDEs exhibit conserved carboxy-terminal catalytic domains, but divergent amino-terminal regulatory regions of varying size. The N-terminal regions enable isotype-specific subcellular localization, as well as responses to different post-translational modifications. PDEs have been recognized as therapeutic targets for a number of diseases, such as erectile dysfunction and pulmonary arterial hypertension (PDE5 inhibitors). The subcellular localization of PDE subtypes allows for compartmentalized degradation of second messenger molecules, and there is evidence to suggest that this principle is critical to their functions in cells. Diffusion of free cAMP is rapid (~400 $\mu m^2/s$)[77], and precise spatiotemporal regulation can only be achieved by a diverse PDE superfamily regulating discrete subcellular compartments.

Catalytic domains of PDEs so far studied by X-ray crystallography demonstrate similar structures of ~350 amino acid residues organized into 16 helices. This active site forms a deep hydrophobic pocket and two binding sites for divalent metal ions essential for catalytic function.

2.7 Phosphodiesterase 4

The cAMP-selective PDE4 family is the largest PDE family, encoding four genes (PDE4A, PDE4B, PDE4C, PDE4D). At least 20 PDE4 gene products are known, with 9 of these stemming from the PDE4D gene (PDE4D1-PDE4D9). One PDE4D, PDE4D3, binds to AKAP450 or mAKAP in cardiac myocytes. In VECs, PDE4 activity accounts for approximately 40% of total cAMP hydrolysis and plays a critical signalling role. All the PDE4D splice variants share a common catalytic domain near the protein's C-terminus. Most splice variants share upstream conserved regions 1 and 2 (UCR1, UCR2), except super-short variants PDE4D2 and PDE4D6, which are missing UCR1 and have partially truncated UCR2[78]. Those variants with N-terminal UCR1 domains include a PKA phosphorylation site, which serves as an activator of enzymatic activity. The long-form variants have unique divergent N-terminal domains that play a role in the protein's subcellular localization and targeting. Interestingly, PDE4D polymorphisms have been found to associate with outcomes of ischemic stroke[79,80], signifying the enzyme's importance for vascular functions.

As a therapeutic target, there are both current and prospective drugs aimed at PDE4. Roflumilast, a PDE4 inhibitor, is licensed for the treatment of chronic obstructive pulmonary disease (COPD). Apremilast, another inhibitor, is licensed for the treatment of psoriatic arthritis. Currently, selective activators of PDE4 short form or long form variants are being developed for conditions such as autosomal dominant polycystic kidney disease (ADPKD). The use of pan-PDE4 inhibitors is limited by severe emetic effects[81]. Hence, searching for a more specific variant to target is worthwhile.

2.8 PDE4D splicing

As detailed above, the multiple distinct mature mRNAs derived from the PDE4D gene each have an identical carboxy-terminal catalytic domain, but diverse significantly in their respective amino-terminal sequences (fig. 4). While they share identical catalytic domains, they differ with respect to the length of their amino-terminal sequences. Indeed, while some encode amino-terminal sequences that contain but upstream conserved region 1 (UCR1) and UCR2, others have more truncated amino termini. The two PDE4D variants of central importance to the current study are PDE4D5 and PDE4D7, both “long-form” splice variants. PDE4D5 has been previously shown to regulate certain VEC signalling events in response to FSS. Yun et al. reported that PDE4D5 directly binds integrin α5 to transduce inflammatory signals in VECs exposed to oscillating FSS[82]. Currently, there are no known binding partners for PDE4D7. Although these findings suggest a role for PDE4D5 in FSS signal transduction, it remains unclear whether PDE4D5 is involved in transducing athero-protective signals as well. Preliminary work by our lab has shown that PDE4D7 is likely involved in VEC adaptation to FSS, making it imperative to explore these two splice variants further.

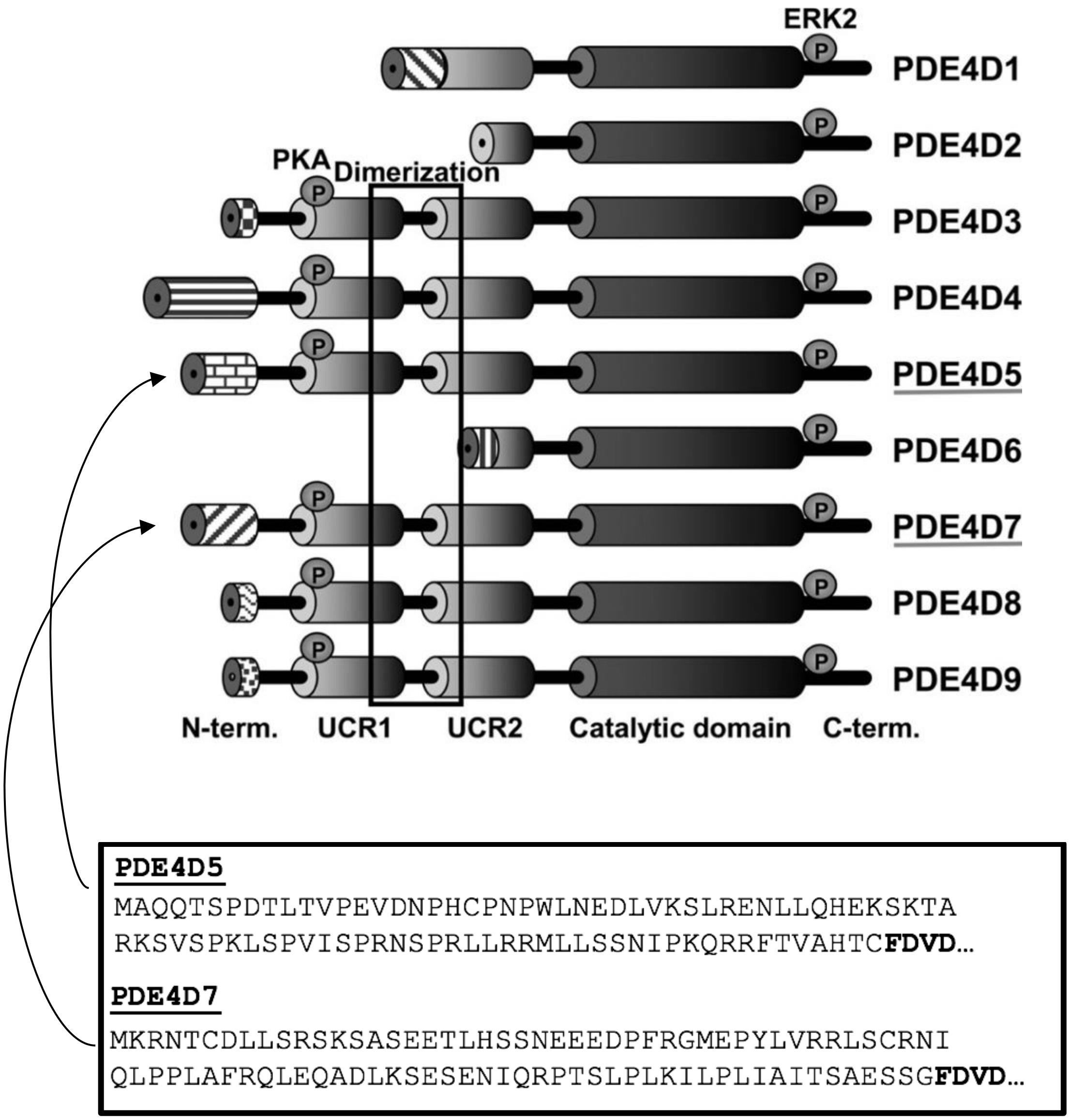

Figure 4. PDE4D splice variants and sequences.

PDE4D splice variants 4D5 and 4D7 differ only in N-terminal sequences. Of note, PDE4D5 and PDE4D7 are the only long-form splice variants expression by VECs, PDE4D4 is absent. Modified from [78]

2.9 cAMP regulation by FSS

There is no a consensus in the literature regarding cAMP signalling in response to FSS. Earlier studies of short-term exposure of HUVECs to FSS (4 dyne/cm^2) reported a 4-fold increase in cAMP when compared to static controls. When application of twisting force with magnetic beads bound to integrin β1- on VECs were used to generate FSS of 20 dyne/cm^2, cAMP increased 3-fold[83]. Blockage of $G\alpha_s$ subunits with guanosine-5'-β-thio-diphosphate (GDP-β-S) attenuated this response, suggesting increases in adenylate cyclase activity were driving increases in cAMP. However, experiments were performed in the presence of pan-PDE inhibitor 3-isobutyl-1-methylxanthine (IBMX), so the role of PDEs in this system remains unclear. In syncytiotrophoblasts, application of FSS increased production of cAMP 3-fold, and also increased phosphorylation of PKA substrates and CREB at S133[84]. In another study, exposure of HUVECs to FSS over 24h resulted in 9-fold decreased global cAMP compared to the static cells, regardless of whether applied FSS was high (75 dyne/cm^2), medium (15 dyne/cm^2) or oscillatory (15 dyne/cm^2)[4]. Another study using bovine aortic endothelial cells, in the presence of IBMX, had no bearing on cAMP levels[85]. A possible explanation for the lack of clear literature regarding FSS-regulated global cAMP levels is that the system does not depend on global cAMP concentrations. Rather, it is plausible that subcellular compartments consistent of differentially regulated pools of cAMP, which work to transduce FSS-encoded signals. The complex involving VE-cadherin, PDE4D and EPAC1 is likely occupies one such compartment.

2.10 Work from our lab: PDE4D tethers and regulates EPAC1

Previous work in our lab performed by Dr. Sarah Rampersad identified a signalling complex that controls VEC response to FSS, and involves the aforementioned PDE4D, EPAC1 and VE-cadherin. First, EPAC1 was identified as the dominant cAMP signaling effector for coordinating permeability-reducing effects of cAMP-elevating agents in VECs. This role is mediated by PDE4D, which functions to tether EPAC1 to VE-cadherin – an interaction that is perturbed by a cell-permeable blocking peptide mimicking the domain with which EPAC1 binds PDE4D[6]. Upon pharmacological inhibition with selective PDE4 inhibitor Ro-20-1724, VEGF-promoted permeability is decreased and EPAC1 is activated. Pulldowns using an immobilized Fc-VE-cadherin chimeric protein and subsequent immunoblots found EPAC1 and PDE4D, as well as Rap1 and PKA-Cα and -RIIβ within a multiprotein complex. The molecular weight of PDE4D (~100 kDa) was consistent with long-form splice variants PDE4D5 and PDE4D7. Using a displacing peptide mimicking the region of EPAC1 from Val-362 to Leu-397, this motif was shown to significantly impact the binding ability of PDE4D. However, it did not displace PDE4D completely, suggesting that PDE4D likely interacts with other members of the complex as well. EPAC1 activation stabilized VE-cadherin borders through Rap1 signaling, an observation that was consistent with previous work by a group in Japan[86].

2.11 PDE4D, EPAC1 and VE-cadherin regulate VEC responses to FSS

In addition to its regulation of permeability, EPAC1 also coordinates the VEC adaptive response to FSS, including alignment and elongation of cells to the direction of flow, and the upregulation of adaptive genes *KLF2*, *eNOS* and *TM*[7]. These three genes are critical response elements to FSS, and important indicators of VEC mechanotransduction of FSS signals. PDE4D is an important regulator of these genes through its role in the same signaling complex. When PDE4D is knocked down with siRNA, VEC adaptive responses to FSS are reduced[8]. PDE4D knockdown impairs both alignment and elongation to FSS, as well as limiting the normal upregulation of *KLF2*, *eNOS* and *TM*. Furthermore, PDE4D and EPAC1 knockdowns reduce the levels of VE-cadherin found at cell borders under both low and high FSS. Taken together, these observations explain the critical roles for this signaling complex in regulating VEC adaptation to FSS.

It is unknown to what extent the actions of PDE4D are mediated through its role as a tether for EPAC1 to VE-cadherin, or by its enzymatic activity hydrolyzing cAMP in subcellular compartments. PDE4D7 has also been implicated in vascular smooth muscle cell (VSMC) migration and tail retraction. It is possible that PDE4D7-targeted therapies might have multiple synergistic effects on improving blood vessel function.

2.12 Research rationale

VECs regulate their phenotype and gene expression in response to FSS from the flowing blood, which determines the locations in the vasculature which are prone to the development of atherosclerosis. Investigating the signaling pathways that act downstream of this mechanical force and which allows it to transduce this force into changes in gene expression and cell behaviours will aid in the identification of therapeutic targets for atherosclerosis.

Previous work by our lab identified the VE-cadherin, PDE4D and EPAC1 signalling complex controlling VEC responses to FSS. PDE4D and EPAC1 were both found to be important in transducing FSS-encoded signals for both morphological alignment to FSS, as well as adaptive gene expression. Further insights regarding the functions of this complex and the pathways it regulates will contribute to our understanding of VEC function and provide new therapeutic targets for VEC dysfunction.

Since PDE4-targeted small molecule inhibitors are limited by emetic effects[9], identifying a more selective and specific target is beneficial. Therefore, ascertaining whether one or more splice variants of PDE4D occupy this signalling complex and control VEC responses to FSS is relevant and pertinent to the field.

2.13 Objectives and hypothesis

First, we sought to evaluate a novel immortalized cell line (teloHAECs) as a model to further investigate the VE-cadherin/EPAC1/PDE4D complex. Studies involving the transfection and selection of cells stably expression a catalytically-dead PDE4D7 construct obviate the need for a cell line capable of unlimited passaging. The teloHAECs were immortalized by overexpressing hTERT, the catalytic subunit of telomerase. This is advantageous over p53- or other oncogene-immortalized cell lines due to maintained genome/karyotype stability. The ATCC, the supplier of the teloHAECs, reported that these cells express several endothelial-like phenotypic markers, but have not assessed responses to FSS. Therefore, we undertook initially to validate their responses to FSS in terms of morphology, gene expression and adherens junction formation. It was our expectation that the teloHAEC cell line would be a valid model of our studies.

Next, we sought to establish the identity of the PDE4D splice variant(s) occupying the aforementioned complex. Previous immunoprecipitation experiments revealed the molecular weight of the PDE4D variant to be consistent with PDE4D5 and PDE4D7. This was explored by selectively knocking down each gene and assessing the expression of adaptive FSS-responsive genes *KLF2*, *eNOS* and *TM*. Considering previous observations that PDE4D7 impairs morphological adaptation to FSS, we hypothesized that PDE4D7 is the splice variant controlling this process and its knockdown will reduce the expression of *KLF2*, *eNOS* and *TM*.

Furthermore, we sought to address the relative importance of catalytic function hydrolyzing cAMP and tethering / scaffolding this complex together. Using teloHAECs, we intended to create stable cell lines expressing catalytically-dead PDE4D7 or full-length GFP-tagged

PDE4D7. If the inactive enzyme displaces the endogenous one from the signalling complex, it will indicate the extent to which it functions as a tether vs. as a cAMP hydrolase for FSS signal transduction.

Lastly, we sought to investigate the effects on FSS-responsive inflammatory mediators such as NF-κB and adhesion molecules ICAM-1 and VCAM-1. Experiments in our lab had focused on transcription factor *KLF2* and two of its gene targets *eNOS* and *TM*. We hoped to clarify whether these effects extend to other FSS-dependent genes. Our hypothesis was that the signaling pathways activated by the VE-cadherin, PDE4D, EPAC1 complex aid in the expression of these inflammatory mediators.

In summary, our objectives were to validate a novel telomerase-immortalized cell line for FSS applications, categorize the splice variant(s) of PDE4D responsible for mediating FSS-encoded signals, and gain insight into how they carry out this function.

Chapter 3

Materials and Methods

3.1 Cell Culture

Human aortic endothelial cells (HAECs) were purchased from Lonza (Walkersville, MD), and telomerase-immortalized human aortic endothelial cells (teloHAECs) were purchased from the ATCC (Manassas, VA). Cells were cultured at 37°C with 5% CO_2, in complete growth media containing 2% fetal bovine serum, 5 ng/mL VEGF, 5 ng/mL FGF, 50 μg/mL ascorbic acid, 1 μg/mL hydrocortisone hemisuccinate, 10 mM glutamine, 15 ng/mL IGF-1, 5 ng/mL EGF, 0.75 U/mL heparin sulfate, 30 mg/mL gentamicin, and 15μg/mL amphotericin B (Lifeline Cell Technologies). Cells were used between passage 4-8 (HAECs) or passage 4-50 (teloHAECs).

3.2 Transfection and RNAi

Cells were incubated with lipofectamine 2000 (Invitrogen) and either negative control or gene-specific siRNA (Ambion) (Table 1) at a 1:1 ratio as per the manufacturer's instructions for 5h in basal media (Lifeline Cell Technologies). RNAi-mediated effects and RNAi-dependent knockdown were evaluated 48 or 72h post-transfection.

Table 1. siRNA sequences

Target	Sense sequence
EPAC1	5′-AUUGAGAUUCUUCUGCUCCUGAGG-3′
PDE4D	5′-GACAAGCACAAUGCUUCCGUGGAAA-3′
PDE4D5	5′-GCUCUCUCCAGUGAUCUCUtt-3′
PDE4D7-1	5′-AGACUUUCAUGUCGCAAUAtt-3′
PDE4D7-2	5′-GAAACACUACAUUCCAGUAtt-3′

3.3 Fluid Shear Stress

Chamber flow slides with 0.4mm height (Ibidi Luer I) were coated by incubation with fibronectin (20 μg/mL) for 1h at 37°C and washed with warm sterile Hank's buffered salt solution (HBSS). Cells were trypsinized for 3 min, counted, and 80,000 cells plated 24h post-transfection in flow slides and incubated for 5h to adhere. Slides were connected to perfusion sets (Ibidi yellow-and-green) and unidirectional flow was applied (Ibidi pump system) for 48h at 3 or 20 dyne/cm^2. Flow rates and corresponding FSS levels were calculated by the Ibidi pump software based on the chamber height and perfusion tubing length and internal diameter, and calibrated using flow rates measured manually in mL/min.

3.4 Imaging

Cells were imaged using brightfield microscopy (Axiovert S100). Images were processed using ImageJ / Fiji macro tool "directionality" Fourier analysis. The tool measures orientation of structures present in the input image by periodic patterning in the Fourier transform of the image. Output values used to calculate alignment index, an in-house metric using the equation:

Alignment index=(Amount/|direction°|/dispersion)*fit*1000.

3.5 Immunofluorescence

Cells were fixed in cold 4% paraformaldehyde for 20 min, washed 3x with HBSS, and blocked with 0.2% BSA in HBSS for 1 hour. Primary antibody (anti-VECAD Bv6, Enzo Life Sciences) was used 1:1000 for 1 hr, and washed with HBSS. Secondary antibody (ie. goat-anti-mouse) was used 1:1000 for 1 hr in combination with nuclear stain (DAPI) and actin stain (phalloidin) at 1:1000 each. Coverslips were mounted in Mowiol, or flow slides were filled with glycerol.

3.6 Gene expression analysis

Following FSS application, RNA was isolated (Qiagen RNeasy Mini Kit) as per manufacturer's instructions, and measured for concentration and purity (NanoDrop 1000, Thermo Fisher Scientific). RNA was reverse transcribed to cDNA (Qiagen Omniscript RT kit) as per manufacturer's instructions to a maximum of 100ng/µl. Gene specific primers (Table 2) were designed (Roche Universal Probe Library) and synthesized (Sigma-Aldrich). Real-time quantitative polymerase chain reaction (RT-qPCR) was performed (QuantStudio5) using SYBR Green-based reagent (PowerUp MasterMix, Thermo Fisher Scientific). PCR was run at 50°C for 2min, 95°C for 10 min, followed by 40 cycles of 95°C for 15s and 59°C for 1 min, ending with 95°C for 15s, 60°C for 1 min, and melt curve analysis at 0.075°C/s to 95°C. Relative quantification of gene expression was calculated using the $\Delta\Delta$-C_t method (Thermo Cloud software), normalized to endogenous control housekeeping genes *PGK1* and *TBP*.

Table 2. RT-qPCR primers

Target	Sense primer	Antisense primer
eNOS	5′-GTGGCTGGTACATGAGCTCT-3′	5′-GTGGTCCACGATGGTGACTT-3′
EPAC1	5′-CGACTGGAGCCTCTTCAACA-3′	5’-CACCCAGTACTGCAGCTCAT-3′
ICAM-1	5′-CGTGGGGAGGAAGGAGCTGAA-3′	5′-CAGTGCGGCACGAGAAATTG-3′
IκB-α	5′-GCTGAAGAAGGAGCGGCTACT-3′	5′-TCGTACTCCTCGTCTTTCATGGA-3′
KLF2	5′-GCAAGACCTACACCAAGAGTTCG-3′	5′-CATGTGCCGTTTCATGTGC-3′
PDE4D	5′-ACGTGGCATGGAGATAAGCC-3′	5′-GTGCTCTGGTACCATTCACGA-3′
PDE4D5	5′-TTTCACGGTGGCACATACAT-3′	5′-GTGGACAAAATTTGCTTGGAG-3′
PDE4D7	5′-TGCCTCTGAGGAAACACT-3′	5′-GCTGAATATTGCGACATG-3′
PGK1	5′-CTGTGGGGGTATTTGAATGG-3′	5′-CTTCCAGGAGCTCCAAACTG-3′
TBP	5′-TATAATCCCAAGCGGTTTGC-3′	5′-GCTGGAAAACCCAACTTCTG-3′
TM	5′-TTGTGGAATTGGGAGCTTGG-3′	5′-TCTCATGAACTGGATGGGGTG-3′
VCAM-1	5′-CATGGAATTCGAACCCAAACA-3′	5′-GACAAGACGGTTGTATCTCTGG-3′

3.7 Statistical analyses

Quantitation of alignment index was analyzed using an unpaired t-test. Relative quantification of genes from biological replicate experiments, calculated from RT-qPCR results, were normalized to the siNegative control siRNA condition. These values were analyzed using a student's two-tailed paired t-test. Values of $p<0.05$ were considered to be statistically significant.

Chapter 4

Results

4.1 Transcriptomic analysis of teloHAECs

Creating stable cell lines expressing constructs with which to study VEC responses to FSS necessitated the use of an immortalized VEC cell line. Therefore, we assessed an immortalized cell line, teloHAECs, as a model for use in some of these studies.

It has been well documented that different cell types throughout the body can have vastly different expression profiles for each of the 11 PDE gene families, with some only being detectable in certain organs or tissues. It was therefore pertinent to consider the relative levels of expression of the PDE4 family of enzymes, particularly germane to our work. Levels of *PDE4* gene transcripts in the teloHAECs and primary HAEC culture were measured and compared by quantitative PCR (qPCR) as described in Materials and Methods. The mRNA expression levels for each of *PDE4A*, *PDE4B* and *PDE4D* genes were not significantly different in these two VECs (figure 5).

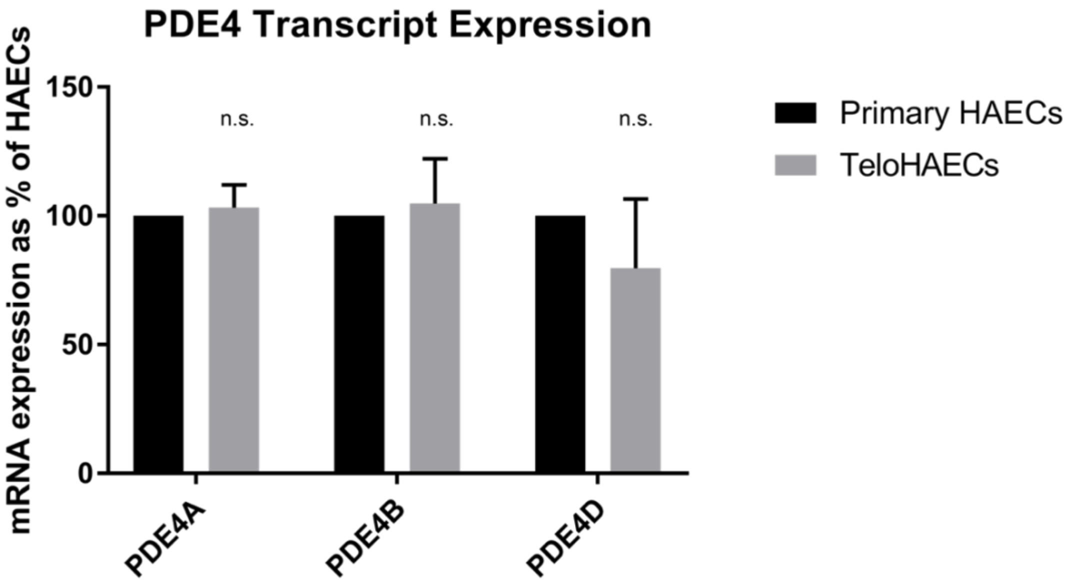

Figure 5. PDE4 transcript expression.

Levels of PDE4A, PDE4B and PDE4D mRNA measured in primary HAECs and teloHAECs by RT-qPCR. Telomerase-immortalized human aortic endothelial cells (teloHAECs) express PDE4A, PDE4B, PDE4D at levels found to be not significantly different from primary HAECs ($p>0.05$) ($n=5$). Data are represented as means normalized to the primary HAECs, +/- SEM error bars.

4.2 Morphological responses of teloHAECs exposed to FSS

The ATCC, from whom the teloHAECs were purchased, indicated in the literature provided on the website that these cells could form tubules and uptake LDL particles and that they expressed cell markers consistent with their annotation as HAECs. In contrast, the responses of these cells to exposure to FSS were not provided in this literature, hence we undertook to assess these responses in our work.

As reported previously, HAECs align and elongate in the direction of flow. In contrast to the case with HAECs, our initial tests of the responses of teloHAECs to FSS indicated that these cells did not align in the direction of flow. Although not rigorously analyzed, we observed that the teloHAECs proliferated more quickly than the primary HAECs, and would continue to proliferate even when confluent. In order to assess whether the different morphological responses to flow that we observed were related to this proliferative difference, we modified our FSS protocol; we decreased the seeding density of teloHAECs from 80,000 cells/slide (that used for HAECs) to 55,000 cells/slide, and reduced the serum concentration from 2% FBS to 0.1 % FBS during flow. These modifications allowed the teloHAECs to align and elongate in the direction to flow (figure 6), although this was not quantitated during these studies.

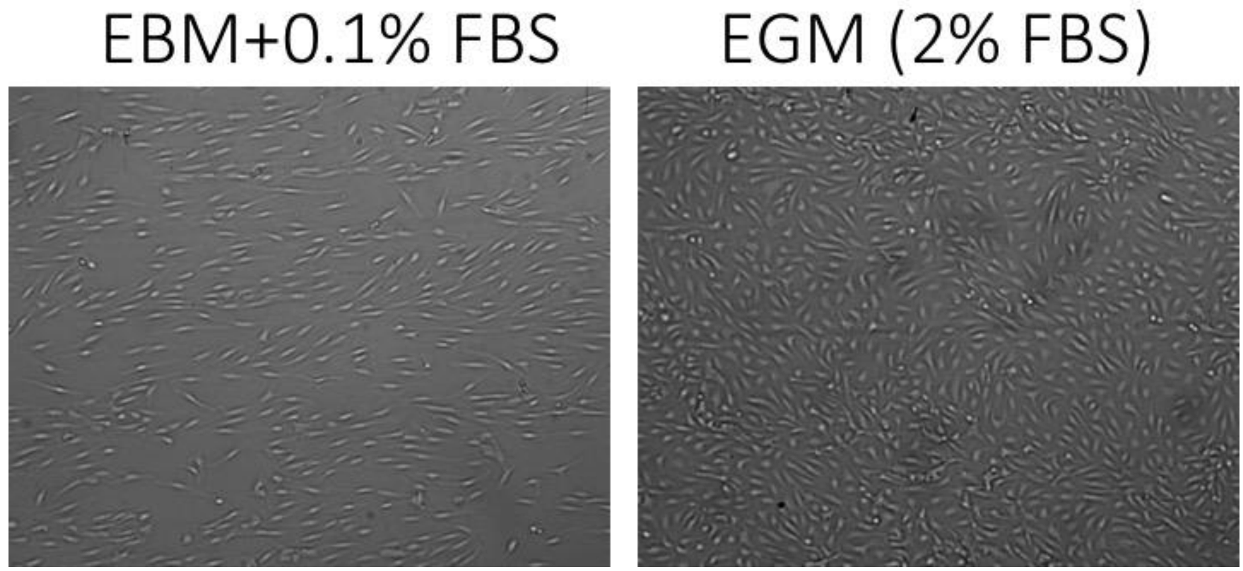

Figure 6. Serum-dependent alignment.

TeloHAEC morphology in basal media vs. complete media. Representative images of cells taken after 48h of exposure to FSS (20 dyne/cm^2). Left: basal media +0.1% FBS. Right: complete growth media + 2% FBS.

4.3 Transcriptomic responses of teloHAECs exposed to FSS

Using our optimized protocol (above), we compared the expression levels of three FSS-regulated genes in teloHAECs cultured under static, low (3 dyne/cm^2) or high (20 dyne/cm^2) FSS for 48h. For these studies, levels of *KLF2*, *eNOS* and *TM* mRNA were measured by PCR and normalized to two housekeeping genes phosphoglycerate kinase 1 (*PGK1*) and TATA binding protein (*TBP*). Our data confirmed that the levels of *KLF2*, *eNOS* and *TM* were increased in a flow-dependent manner (figure 7), consistent with previous observations in primary HAECs.

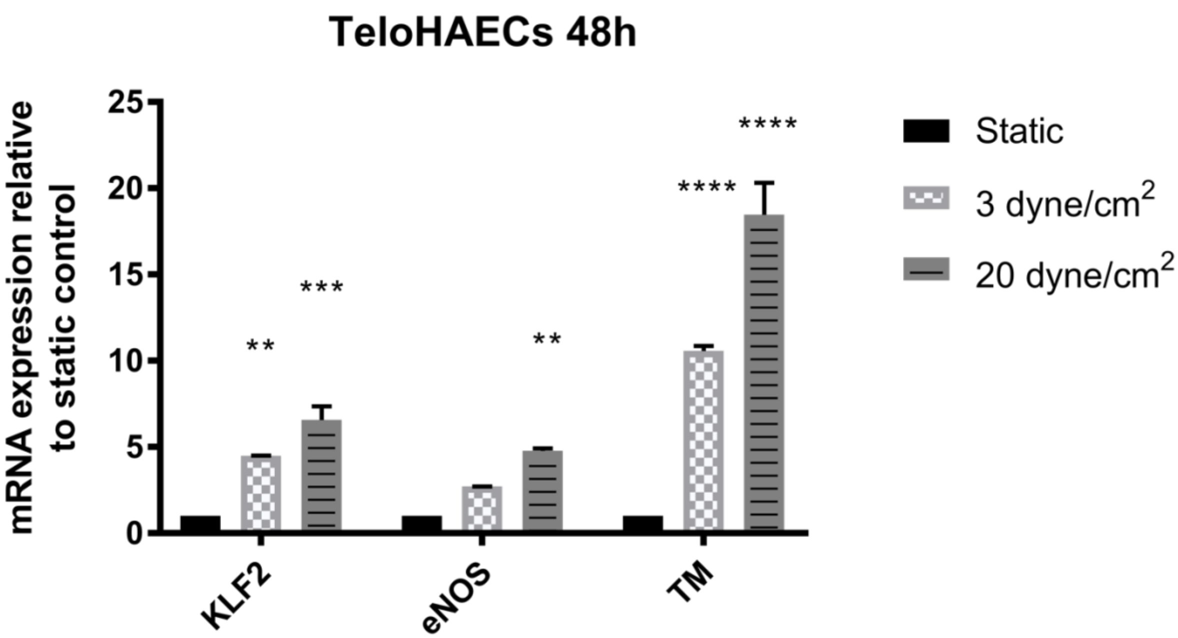

Figure 7. TeloHAEC transcriptional response to FSS.

Levels of *KLF2*, *eNOS* and *TM* in teloHAECs exposed to low (3 dyne/cm^2) or high (20 dyne/cm^2) FSS for 48h were measured by RT-qPCR and are normalized to the static controls. Student's t-tests were used to determine statistical differences. Data are means +/- SEM error bars,
(** $p<0.01$, ***$p<0.001$, ****$p<0.0001$, n=3).

4.4 Adherens junctions in teloHAEC cultures

Formation and dynamic regulation of contiguous cell contacts enriched in adherens junctional proteins are prerequisites for the VE-cadherin-based mechanosensory complex we wish to explore in these studies. To further validate teloHAECs as a model, we assessed their ability to form said VE-cadherin-enriched border structures subsequent to their exposure to FSS for 48h (20 dyne/cm^2). Staining indicated that these cells did form adherens junctions and that these were in close apposition with cortical actin fibres similar to those observed in HAECs similarly treated (figure 8).

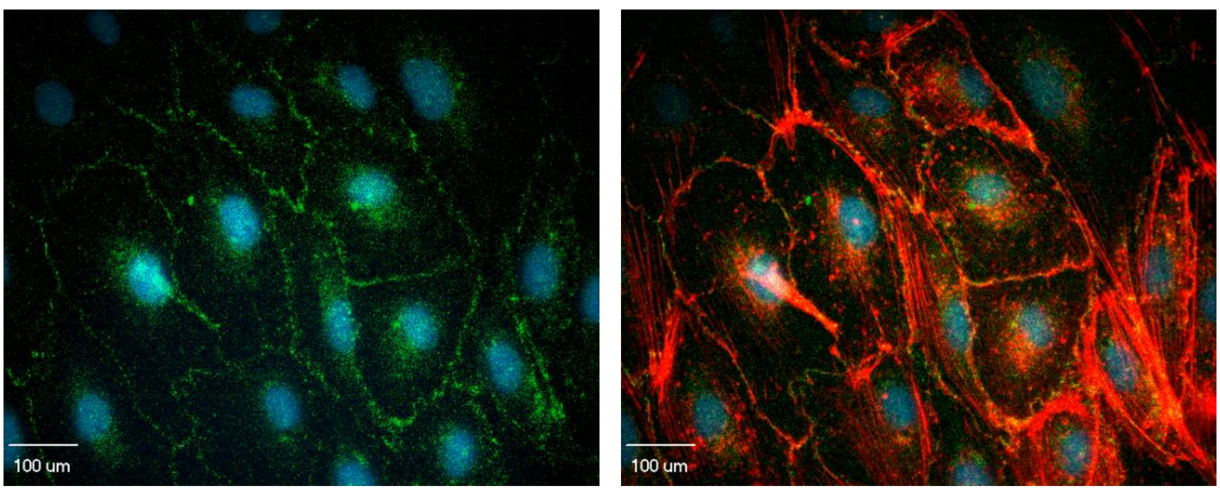

Figure 8. TeloHAECs have VE-cadherin-enriched cell borders.

Representative images of teloHAECs stained for nuclei (DAPI, blue), VE-cadherin (anti-Vecad-BV6, green) (left) and F-actin (phalloidin, red) (right). Images taken at 20x magnification.

4.5 Knockdown efficiency of siRNAs used in this study

In each RT-qPCR analysis of changes in gene expression, levels of expression the relevant gene being knocked down were assessed. In this study, siRNAs were used targeting EPAC1, PDE4D, PDE4D5 and PDE4D7. Reductions in mRNA expression of 60-80% were achieved (figure 22).

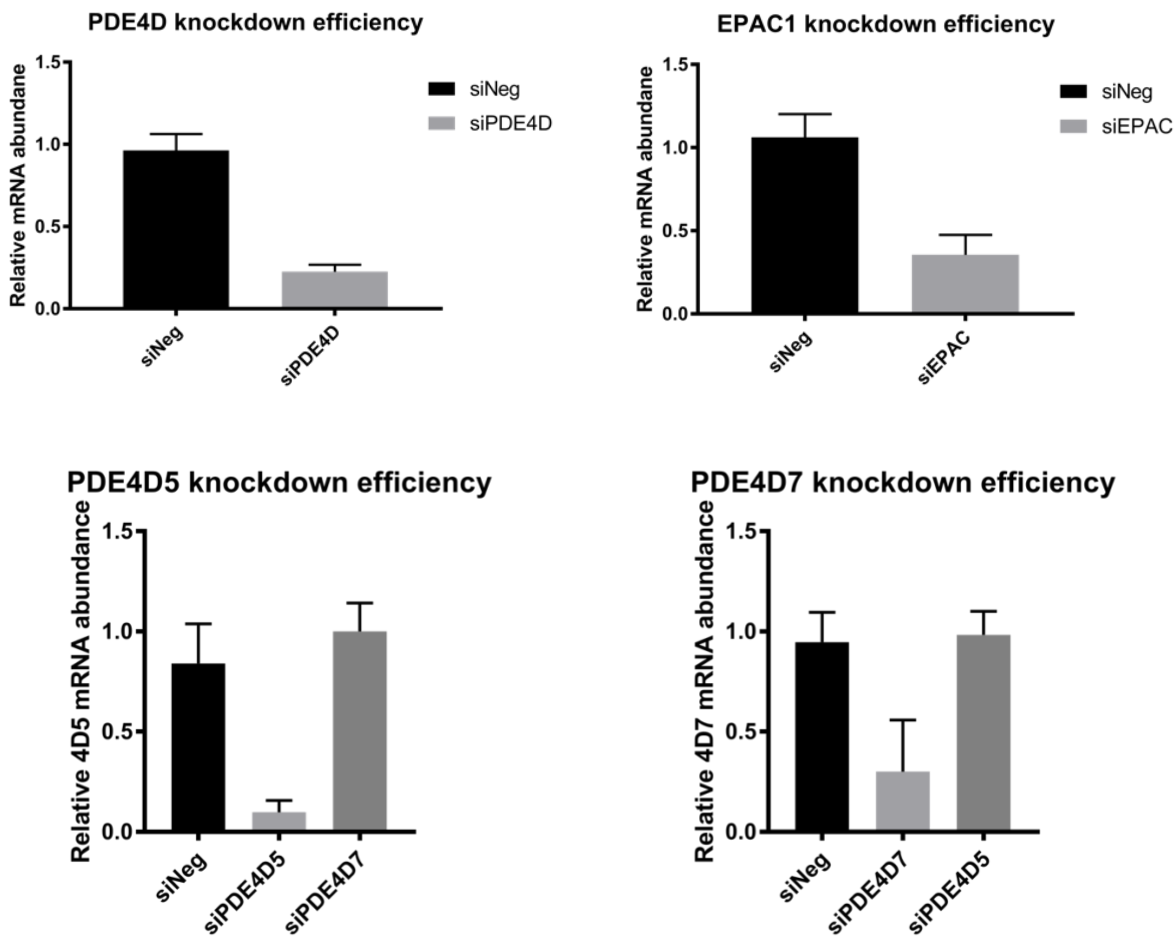

Figure 9. Knockdown efficiency of siRNAs.

Relative abundance of target genes assessed by RT-qPCR. Data are means +/- SEM error bars. n=3-8.

4.6 PDE4D7 knockdown impairs teloHAEC adaptive responses to FSS

Preliminary data collected by Dr. Rampersad and our lab previously suggested that knocking down the level of expression of the *PDE4D* variant *PDE4D7* reduced the morphological responses of VECs to FSS. To confirm and further address this, we chose to investigate the effects of PDE4D7 knockdown on morphological and transcriptomic responses of these cells. Thus, teloHAECs were subjected to 0, 3 or 20 dyne/cm^2 FSS for 48h and imaged with a brightfield microscope. TeloHAEC alignment was quantified using our in-house method of calculating alignment index, based on measurements taken by the Fiji (ImageJ) plugin "directionality" (Fourier analysis). We observed that teloHAECs subjected to FSS aligned in the direction of flow and that the magnitude of this effect was greater at higher levels of FSS. In addition, we observed that knocking down PDE4D7 significantly reduced the ability of these cells to align in the direction of flow (figure 10). These results were consistent with our expectations based on previous observations of PDE4D7-knockdown primary HAECs (Rampersad, unpublished).

After considering the impact of PDE4D7 on morphological adaptation to FSS, we next assessed the effect of PDE4D7 knockdown on adaptive gene expression in teloHAECs. Thus, while the levels of *KLF2*, *eNOS* and *TM* were each markedly increased by FSS in these cells, those responses were reduced in cells where PDE4D7 had been silenced (figure 11).

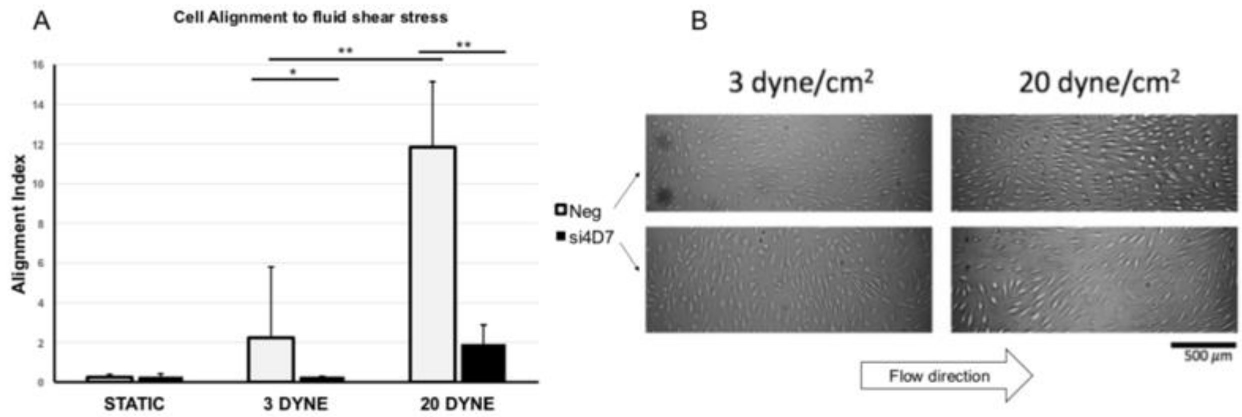

Figure 10. PDE4D7 knockdown impairs alignment to FSS.

TeloHAECs were transfected with control siRNA (Neg) or siRNA for PDE4D7 (si4D7) and exposed to low (3 dyne/cm^2) or high (20 dyne/cm^2) FSS for 48h, and imaged. A. Images analyzed by ImageJ alignment macro using Fourier components, and output values calculated into alignment index. Alignment index =(Amount/|direction°|/dispersion)*fit*1000. SEM error bars, n≥5 or greater for each condition, p<0.05 for * and p<0.01 for **. B. Representative images of flowed cells (teloHAECs) after 48h of low or high laminar (3 or 20 dyne/cm^2 respectively) fluid shear stress.

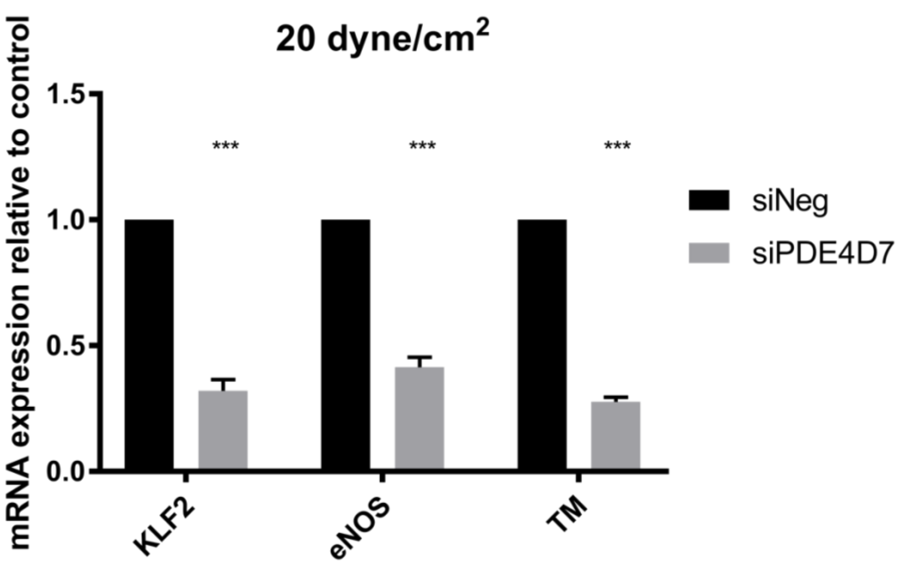

Figure 11. PDE4D7 knockdown impairs adaptive gene expression in response to FSS.

Levels of *KLF2*, *eNOS* and *TM* mRNA in teloHAECs transfected with a control siRNA (siNeg) or with a PDE4D7 siRNA, and subjected to high laminar (20 dyne/cm^2) FSS for 48h, were measured by RT-qPCR. Student's t-tests were used to detect significant differences between control and PDE4D7 knockdown cells for each separate experiment (n=3, ***p<0.001). Data are means +/- SEM error bars.

4.7 Reproducing EPAC1 and PDE4D mediated effects in teloHAECs

As noted, Dr. Rampersad had showed previously that EPAC1 and PDE4D each were present in a VE-Cadherin-based complex in HAECs and that their actions within this complex regulated their responses to FSS[6]. Thus, before continuing our studies further, and moving on to the creation of stable cell lines expressing altered EPAC1 and PDE4D variants using these cells, we further attempted to replicate previous experiments using the pan-PDE4D and EPAC1 siRNAs used previously by Dr. Rampersad in the teloHAECs. To our surprise, while these cells responded adaptively to FSS, and PDE4D7 knockdown inhibited these effects, expression levels of *KLF2*, *eNOS* or *TM* in cells in which either EPAC1 or pan-PDE4D, remained unchanged when normalized with housekeeping genes *PGK1* and *TBP*. Surprisingly, PDE4D or EPAC1 knockdown in teloHAECs did not yield any significant changes in the expression of *KLF2*, *eNOS* or *TM* (figure 12, 13).

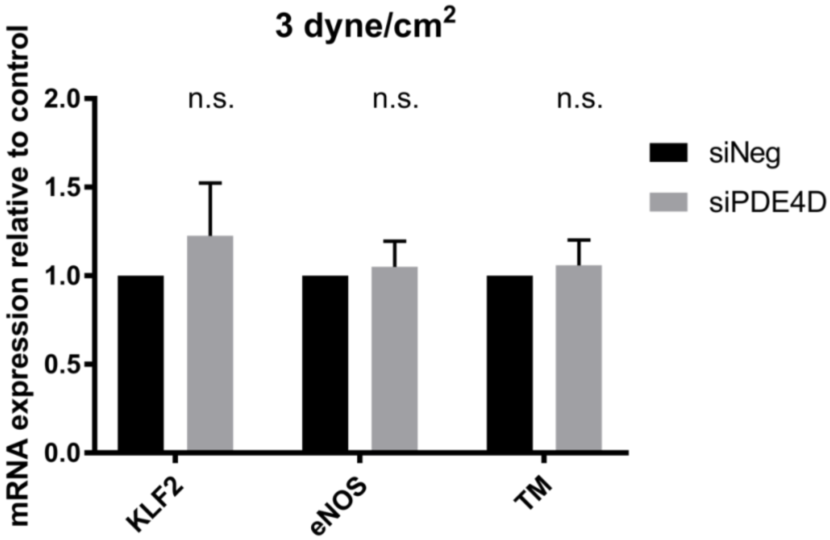

Figure 12. Adaptive gene expression in PDE4D knockdown teloHAECs.

TeloHAECs with siRNA PDE4D knockdown do not have impaired *eNOS*, *KLF2* and *TM* upregulation in response to FSS as was previously observed with primary HAECs exposed to low laminar (3 dyne/cm^2) FSS for 48h, compared to siNegative controls. Data shown are means with SEM error bars. Paired t-test, $p>0.05$, $n=2$.

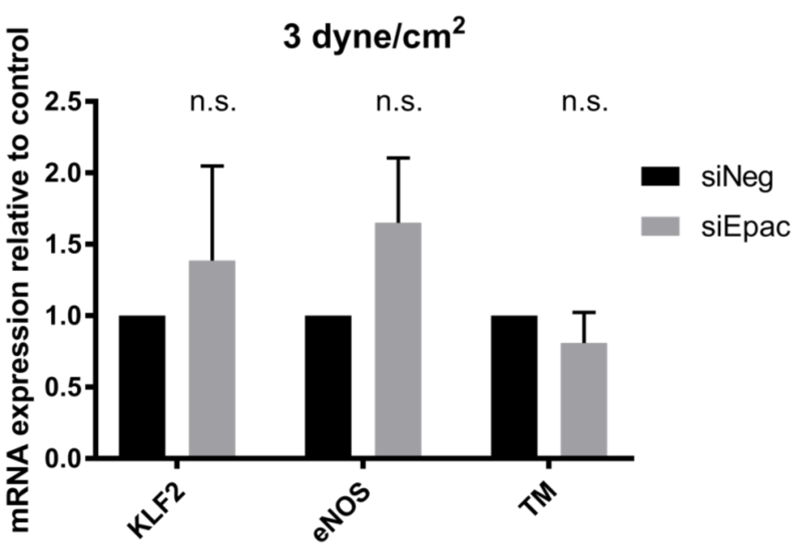

Figure 13. Adaptive gene expression in EPAC1 knockdown teloHAECs.

Levels of *KLF2*, *eNOS* and *TM* were measured in teloHAECs with siRNA EPAC1 knockdown exposed to low laminar (3 dyne/cm^2) FSS for 48h, compared to siNegative controls. Data shown are means with SEM error bars. Paired t-test, $p>0.05$, $n=2$.

4.8 Replicating previous observations in primary HAECs

Based on the data collected thus far, it had appeared as though teloHAECs were a suitable model for use in future experiments. However, following the failure to replicate these important PDE4D- and EPAC1-mediated effects on adaptive response to FSS in the teloHAECs, we elected to return to using primary HAECs to reproduce these effects. These cells were exposed to either low (3 dyne/cm2) or high (20 dyne/cm2) FSS and RNA extracted. RT-qPCR assessed the expression of *KLF2*, *eNOS* and *TM* as well as *PGK1* and *TBP*. As expected, and consistent with previous observations in the same cell type, the expression of *KLF2*, *eNOS* and *TM* was reduced in HAECs where either PDE4D or EPAC1 had been knocked down, following 48h exposure to FSS. (figure 14, 15).

Having returned to using primary cells as our model, it became impossible to generate stable endothelial cell line-based approaches to address the role of PDE4D7. Therefore, in order to determine whether or not PDE4D7 was the dominant long-form PDE4D splice variant in the VE-cadherin-based complex regulating VEC response to FSS, we conducted targeted knockdowns of either PDE4D7 or PDE4D5, the only two PDE4D splice variants with a molecular weight consistent with previous immunoprecipitation experiments[6]. Based on previous observations, we predicted that PDE4D7 was the dominant PDE4D splice variant controlling FSS responses in the VE-cadherin-EPAC1-associated multiprotein complex.

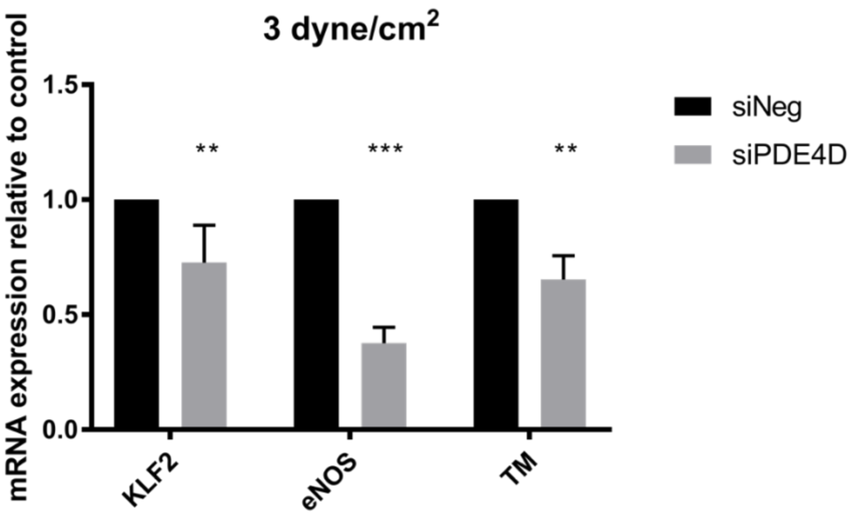

Figure 14. Adaptive gene expression in PDE4D knockdown HAECs after low flow.

Levels of *KLF2*, *eNOS* and *TM* in HAECs transfected with control siRNA (siNeg) or with a pan-PDE4D siRNA exposed to low laminar (3 dyne/cm^2) FSS for 48h measured by RT-qPCR. Student's t-tests were used to determine statistical differences between control and PDE4D knockdown cells. Data shown are means with SEM error bars. n=2, **p<0.01, *** p<0.001.

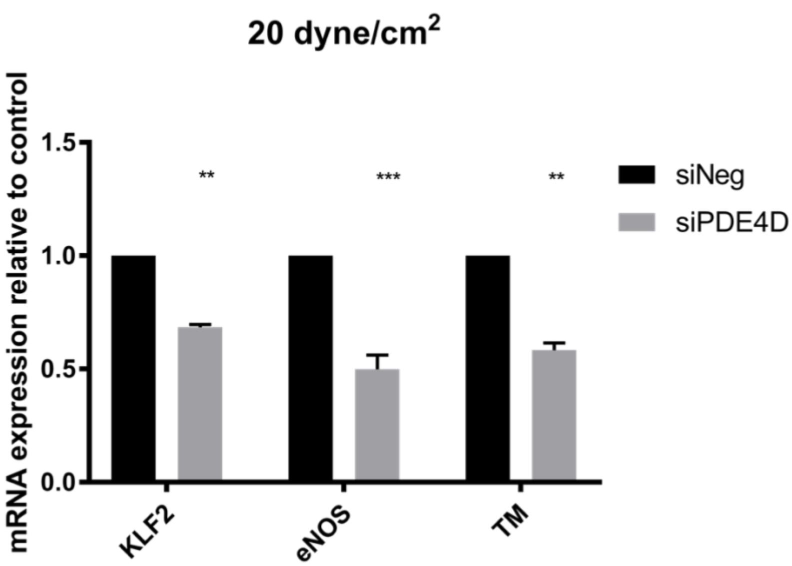

Figure 15. Adaptive gene expression in PDE4D knockdown HAECs after high flow.

Levels of *KLF2*, *eNOS* and *TM* in HAECs transfected with control siRNA (siNeg) or with a pan-PDE4D siRNA exposed to high laminar (20 dyne/cm^2) FSS for 48h measured by RT-qPCR. Student's t-tests were used to determine statistical differences between control and PDE4D knockdown cells. Data shown are means with SEM error bars. n=2, **p<0.01, *** p<0.001.

4.9 Determination of PDE4D splice variant selectivity in VEC response to FSS

For these studies, HAECs were transfected with siRNA for PDE4D7, plated on fibronectin-coated flow slides, and exposed to 48h of low or high FSS, as described in Materials and Methods. Following flow, RNA was extracted, reverse transcribed and used in qPCR reactions to monitor the expression of *KLF2, eNOS*, *TM*, *PGK1* and *TBP*, as described in Materials and Methods. Based on these experiments, we observed that PDE4D7 selective silencing markedly reduced the expression of *KLF2, eNOS* and *TM* in response to FSS at both 3 dyne/cm^2 (figure 16) and 20 dyne/cm^2 (figure 17). In marked contrast, silencing of the other PDE4D variant, PDE4D5, we observe no effect on the flow-induced changes in the expression of any of these adaptive genes, either at 3 dyne/cm^2 (figure 18) or 20 dyne/cm^2 (figure 19). These results suggest, consistent with our hypothesis, that PDE4D7 and not PDE4D5 regulates adaptive VEC responses to FSS.

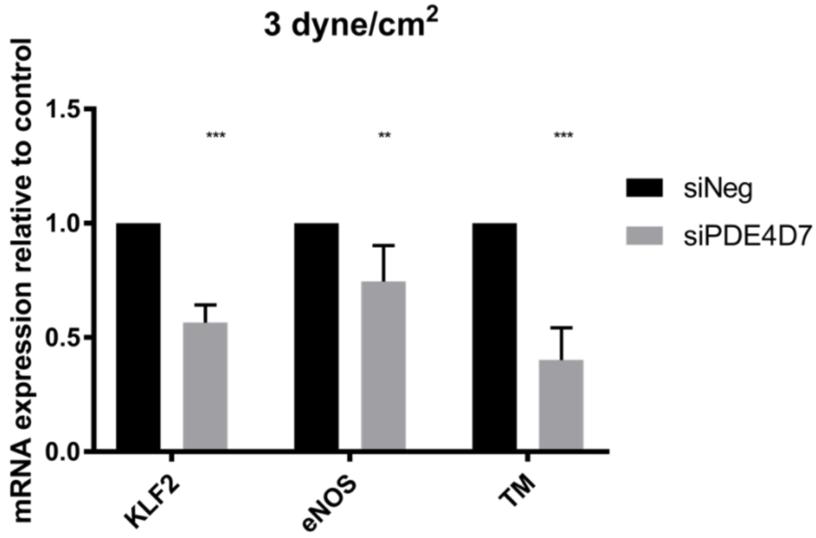

Figure 16. Adaptive gene expression in PDE4D7 knockdown HAECs after low flow.

Levels of *KLF2*, *eNOS* and *TM* in HAECs transfected with control siRNA (siNeg) or with a PDE4D7 siRNA exposed to low laminar (3 dyne/cm^2) FSS for 48h measured by RT-qPCR. Student's t-tests were used to determine statistical differences between control and PDE4D7 knockdown cells. Data shown are means with SEM error bars. n=5, **p<0.01, *** p<0.001.

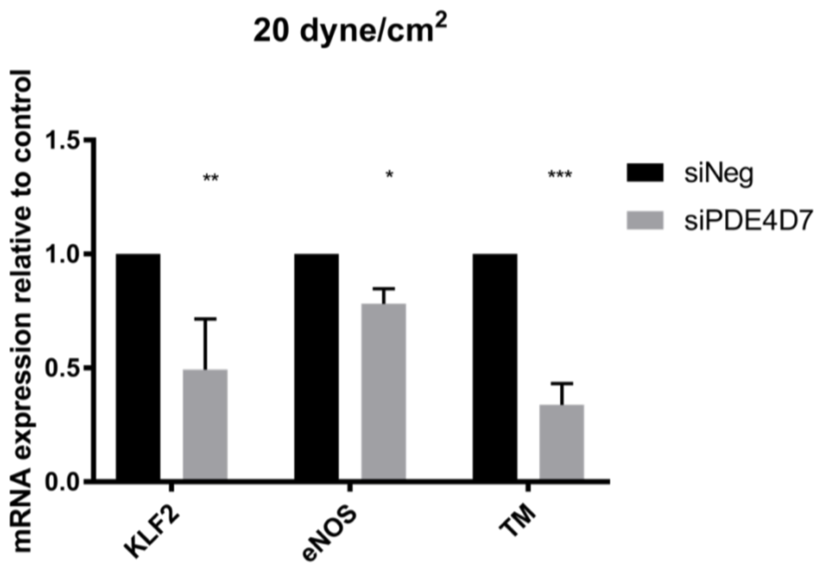

Figure 17. Adaptive gene expression in PDE4D7 knockdown HAECs after high flow.

Levels of *KLF2*, *eNOS* and *TM* in HAECs transfected with control siRNA (siNeg) or with a PDE4D7 siRNA exposed to high laminar (20 dyne/cm^2) FSS for 48h measured by RT-qPCR. Student's t-tests were used to determine statistical differences between control and PDE4D7 knockdown cells. Data shown are means with SEM error bars. n=3, *p<0.05, **p<0.01, *** p<0.001.

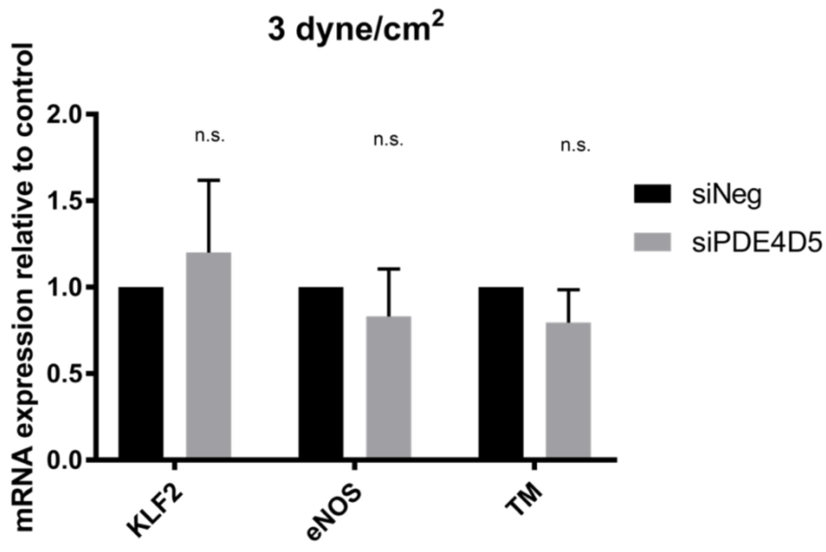

Figure 18. Adaptive gene expression in PDE4D5 knockdown HAECs after low flow.

Levels of *KLF2*, *eNOS* and *TM* in HAECs transfected with control siRNA (siNeg) or with a PDE4D5 siRNA exposed to high laminar (3 dyne/cm^2) FSS for 48h measured by RT-qPCR. Student's t-tests were used to determine statistical differences between control and PDE4D5 knockdown cells. Data shown are means with SEM error bars. n=5, p>0.05

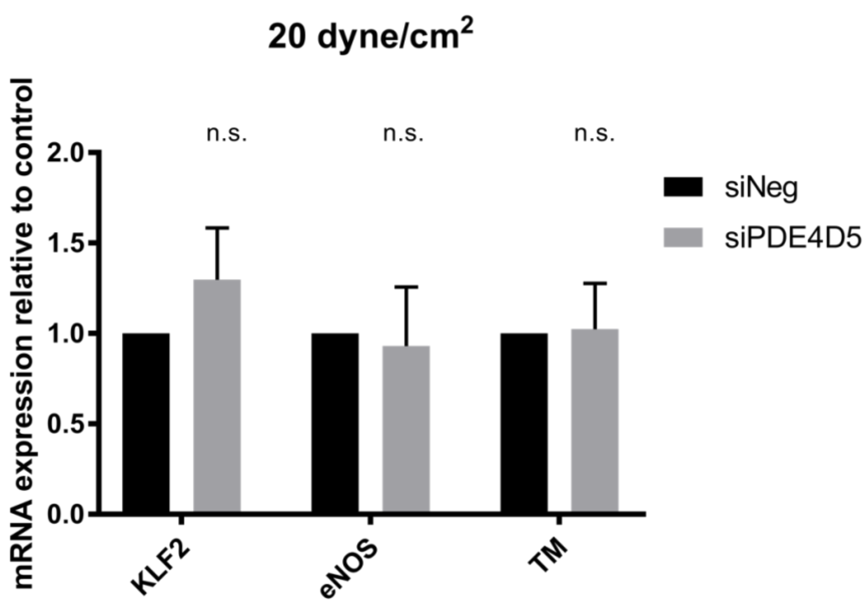

Figure 19. Adaptive gene expression in PDE4D5 knockdown HAECs after high flow.

HAECs with siRNA PDE4D5 knockdown do not have impaired *eNOS*, *KLF2* and *TM* upregulation in response to 20 dyne/cm^2 FSS for 48h, compared to siNegative controls. Data shown are means with SEM error bars. Paired t-test, p>0.05, n=4.

4.10 Expression of inflammatory markers

In addition to assessing adaptive markers of VEC FSS response *KLF2*, *eNOS* and *TM*, the expression of the inhibitory subunit of NF-kB (IκB-α), as well as adhesion molecules ICAM-1 and VCAM-1 were also measured. Selectively silencing either PDE4D5 or PDE4D7 in HAECs did not influence the basal levels of these genes when cells were cultured without flow under static conditions (figure 20). In contrast, when HAECs in which PDE4D5 had been silenced were exposed to 3 dyne/cm^2 FSS for 48h, there was a statistically significant increase of IκB-α compared to siNegative controls (figure 21). When these siPDE4D5 cells were exposed to high laminar FSS (20 dyne/cm^2) FSS for 48h, expression levels of VCAM-1 were reduced significantly compared to the siNegative controls. Similarly, when PDE4D7-knockdown cells were cultured under high laminar FSS (20 dyne/cm^2), VCAM-1 transcript levels were similarly reduced (figure 22). There were no other significantly different changes in expression of IκB-α, ICAM-1 or VCAM-1.

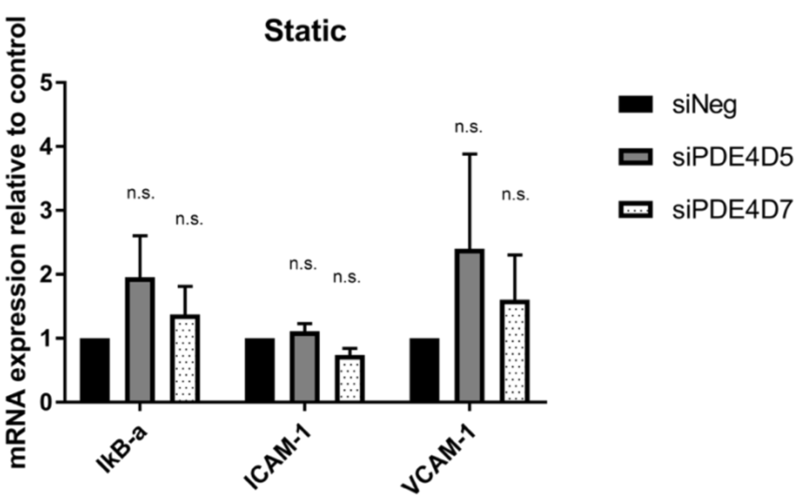

Figure 20. Expression of inflammatory markers in static HAECs.

Levels of expression of IκB-α, ICAM-1 and VCAM-1 in HAECs transfected with control siRNA (siNeg) or siRNA for PDE4D5 or PDE4D7, measured by RT-qPCR. Data shown are means +/- SEM error bars. Paired t-test, $p>0.05$, $n=3$.

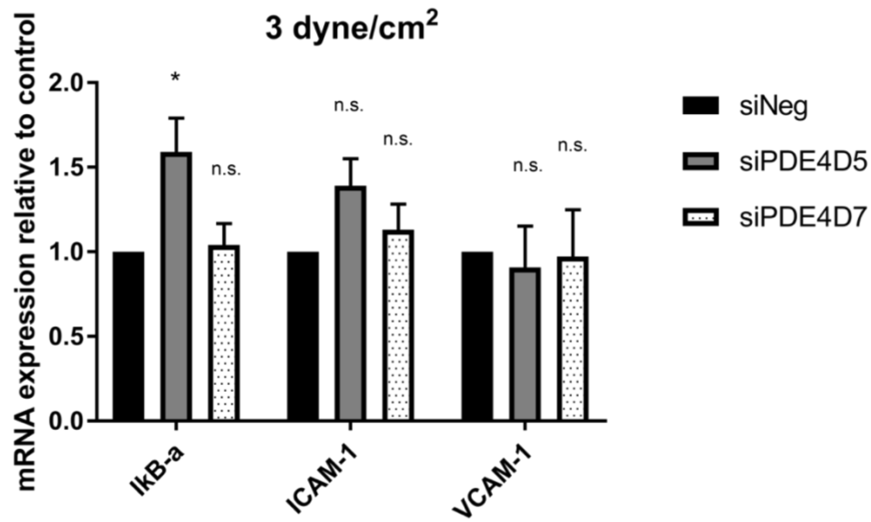

Figure 21. Expression of inflammatory markers in HAECs after low flow.

Levels of expression of IκB-α, ICAM-1 and VCAM-1 in HAECs transfected with control siRNA (siNeg) or siRNA for PDE4D5 or PDE4D7, exposed to low laminar (3 dyne/cm^2) FSS for 48h, measured by RT-qPCR. Student's t-tests were used to determine statistical significance. Data shown are means +/- SEM error bars. *p<0.05, n=3

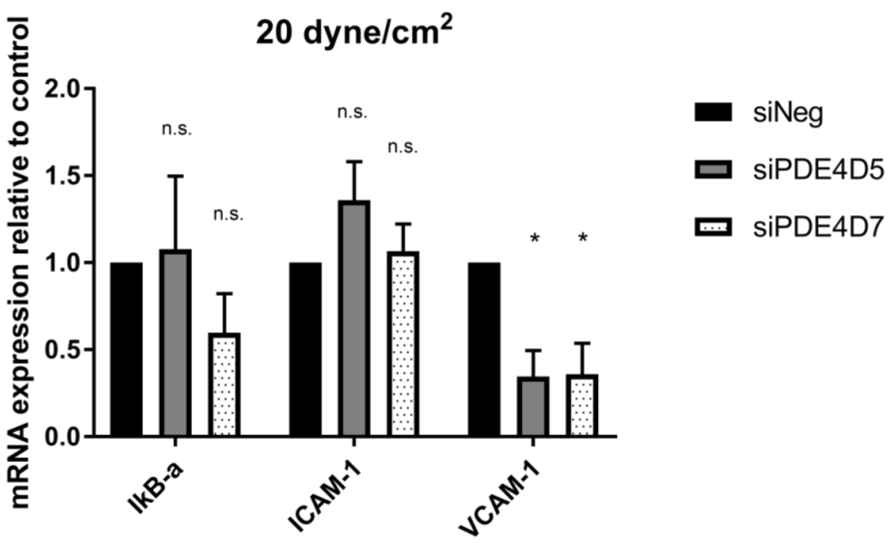

Figure 22. Expression of inflammatory markers in HAECs after high flow.

Levels of expression of IκB-α, ICAM-1 and VCAM-1 in HAECs transfected with control siRNA (siNeg) or siRNA for PDE4D5 or PDE4D7, exposed to high laminar 20 dyne/cm^2 FSS for 48h, measured by RT-qPCR. Student's t-tests were used to determine statistical significance. Data shown are means +/- SEM error bars. *p<0.05, n=3

Chapter 5

Discussion

5.1 Summary of Findings

Understanding the process by which VECs transduce FSS-encoded mechanical stimuli into biochemical signals may be key to developing effective therapies to target the development or progression of atherosclerosis at the level of VEC dysfunction. In the work described in this thesis, I set out to extend upon earlier studies[6-8] done by Dr. Sarah Rampersad in the Maurice lab prior to my arrival. As previously described, Dr. Rampersad had identified and characterized a multi-protein signaling complex containing several adherens junctions proteins (VE-cadherin, β-catenin), a PDE4D, and cAMP effector EPAC1. Moreover, she had found that this complex allowed cAMP to influence VEC responses to FSS. Most interestingly, she showed that PDE4D had two functions in this system: first, that it hydrolyzed cAMP and in doing so controlled EPAC1 activity, and second, that it served as a tether for EPAC1 integration into the multiprotein complex. My studies were planned to allow me to assess which of these two functions of PDE4D played a dominant role in allowing it to regulate EPAC1-mediated effects on VEC responses to FSS, and to identify the PDE4D variant(s) that formed part of this complex.

As described, I initially set out to use telomerase-immortalized HAECs (teloHAECs) for my studies, since they offered several advantages over primary HAEC cultures, including their potential to support the creation of stable cell lines. While I observed that teloHAECs behaved similarly to primary HAEC cultures in many ways, including their ability to modulate their morphology and their transcriptome in response to FSS, their responses were not ideal for out purposes. Most notably, knocking down either PDE4D or EPAC1 did not recapitulate effects observed in the primary HAECs. While silencing either PDE4D or EPAC1 attenuated adaptive gene expression of *KLF2*, *eNOS* and *TM* in HAECs exposed to FSS[7,8], these effects were not observed in teloHAECs. Given that these observations formed the basis of my studies, it became clear that teloHAECs were unsuitable for studying this system.

Reverting to the primary HAECs model used previously, I investigated the influence of selectively knocking down PDE4D5 or PDE4D7 on the responses of these cells to FSS. My data showed that knocking down PDE4D7, but not PDE4D5, impaired adaptive gene expression in response to FSS. These data are consistent with the idea that PDE4D7 is the splice variant acting as a tether for EPAC1 in a complex with VE-cadherin (fig. 12). These findings identify PDE4D7 as the relevant PDE4D splice variant that would be target by potential therapies for VEC dysfunction and atherosclerosis.

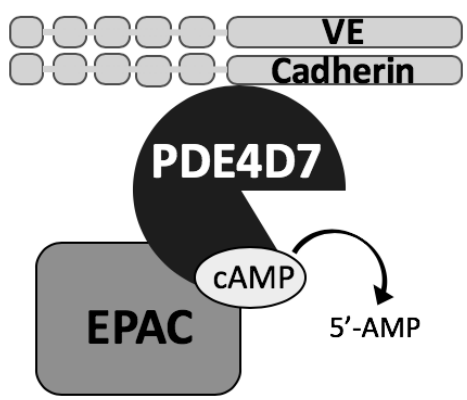

Figure 23. PDE4D7 based complex with EPAC and VE-cadherin.

5.2 Evaluation of teloHAECs as a model

In order to comprehensively investigate how PDE4D regulates EPAC1-mediated FSS responses in HAECs, we had initially planned to manipulate the expression and activity of the two PDE4D variants expressed by teloHAECs, PDE4D5 and PDE4D7. Our approach would have involved heterologous expression of catalytically-inactive PDE4D constructs, and utilized the CRISPR-cas9 gene editing system to selectively abolish their expression. Since primary HAECs have a very limited life span in culture, we obtained immortalized teloHAECs for these studies. In order to proceed, functionally validating that these cells would serve as a valid model for the primary HAECs was necessary.

First, we compared PDE4 the expression in primary and teloHAECs by RT-qPCR using reverse transcribed mRNAs. Since different cells can have vastly divergent PDE expression patterns, this represented a critical initial step in my studies. My results were entirely consistent with the idea that levels of PDE4A, PDE4B and PDE4D expression in the primary HAEC and teloHAEC cultures were indistinguishable.

The source of our teloHAECs (ATCC) reported in the literature that the cells retained certain VEC-specific characteristics, including CD-31/PECAM-1 expression, LDL functional uptake, inflammatory response to TNF-α, proliferation upon VEGF stimulation, and importantly, neo-angiogenesis and tube formation[87]. In contrast, the proliferative characteristics of these cells and their ability to respond to FSS had not been previously assessed. Notably, these immortalized cells grew at a faster rate compared to the primary culture. This necessitated that I spend a significant amount of time optimizing the seeding density and compare the responses of these cells in the presence or absence of serum. In the presence of serum during the application of FSS, teloHAECs did not align and elongate to the extent seen routinely in the primary HAECs. This may have been due to the increased proliferative nature of these cells, which allowed them to become over-confluent if not adjusted for. Although not tested directly, hyper-proliferation due to serum presence possibly inhibited these cells from aligning to flow. Removal of serum allowed teloHAECs to align and elongate in response to FSS, suggesting that they could still function as a valid model of primary HAECs.

We were also unsure of the ability of the teloHAECs to form contiguous borders enriched with VE-cadherin, especially given this hyperproliferative phenotype. In teloHAECs exposed to FSS as well as static controls, immunostaining with antiserum for VE-cadherin established that these cells do in fact make such borders, consistent with the observations in the primary culture. Although there were differences in proliferative capacity, which is not unexpected of telomerase-immortalized cells, the responses to FSS thus far had been consistent with primary HAECs and indicative that teloHAECs would serve as an accurate VEC model.

There has not been any literature reporting the use teloHAECs for FSS-related applications. Therefore, it was necessary to investigate whether the teloHAECs could respond to FSS in a manner similar to that reported by us for primary HAEC cultures, and whether the protocols established for those cells would be applicable. The expression of the genes *KLF2*, *eNOS* and *TM* are upregulated in a flow-dependent manner in primary HAECs as well as other VECs, so we expected teloHAECs to behave in the same way. Analysis of relative gene transcript expression in teloHAECs exposed to low or high FSS confirmed that they upregulate *KLF2*, *eNOS* and *TM* in a manner consistent with previous observations in other cell types. These findings indicated that the teloHAECs were capable of transducing FSS signals into transcriptional responses typical of VECs.

Having established conditions in which teloHAECs respond to FSS, I then set out to replicate two key observations first reported by Dr. Rampersad: that the adaptive increase in expression of *KLF2*, *eNOS* and *TM* in response to FSS was reduced by siRNA knockdown of PDE4D or EPAC1. We expected the teloHAECs to behave in a manner consistent with the primary HAECs, and have reduced levels of *KLF2*, *eNOS* and *TM* when PDE4D or EPAC1 are knocked down. Based on the importance of PDE4D and EPAC1 in response to FSS our lab observed previously, we would expect all large artery derived VECs to rely on these proteins to a similar extent. To my dismay, we could not replicate these findings in this cell line, either under identical conditions or with teloHAEC-optimized serum-free conditions. Even with good knockdown efficiency (70-80%), the effects previously observed and published were not reproducible in the immortalized VECs.

While the basis of this discrepancy is not known, it is possible that the clonal nature of teloHAECs could be important. Indeed, while primary HAEC cultures are necessarily heterogenous, and contain individual HAECs with numerous distinct phenotypes, our teloHAEC clone necessarily represents the phenotype of a single VEC from the population of hTERT-expressing cells. For instance, it is known that the von Willebrand factor (vWF) gene is expressed in a dynamic mosaic pattern and switches on and off stochastically[88]. This may be the case for expression of other endothelial cell proteins as well, a pattern which would likely be altered by selecting a single clone from a population.

Another, more direct explanation for differences between teloHAECs and primary HAECs is the overexpressed hTERT itself. Although hTERT-immortalized cell lines are regarded as superior to oncogene-immortalized cell lines due to their relatively stable genomic structures, there are still numerous off-target effects that might impact the phenotype and behaviour of the cells. Thus, it is possible that increased telomerase activity resulting from the abundant hTERT includes unintentional changes to cell function. For instance, hTERT is a target of the Wnt/β-catenin signalling pathway[89], and may feedback to regulate its signalling in unforeseen ways. It has also been reported that hTERT has noncanonical functions regulating the expression of certain genes, in an indirect and cell-type-dependent fashion[90]. One study found that hTERT expression significantly increases cell adhesion and migration[91]. Another study found that hTERT overexpression alleviates ROS production, and improved mitochondrial function[92]. The PI3K/Akt pathway is important in transducing FSS-encoded signals, and it is up-regulated by hTERT overexpression as well[90]. These pathways and functions are either directly or indirectly involved in FSS signal transduction, and their modulation by hTERT overexpression may impact FSS responses. Perhaps, then, it should not have been so surprising that certain results from primary HAECs were not reproducible in teloHAECs.

5.3 Knockdown of PDE4D7 impairs adaptive responses to FSS

Given that PDE4D and EPAC1 mediated effects were not observed in teloHAECs, it was not a priority to proceed with experiments using that cell line. One of the main goals of this study was to identify the splice variant of PDE4D responsible for transducing FSS-encoded adaptive signals, feasible in primary HAECs. Based on previous morphological observations after PDE4D7 knockdown, we hypothesized that PDE4D7 was acting as the dominant splice variant of PDE4D in transducing FSS signals in VECs. Therefore, we expected that siRNA-mediated knockdown of PDE4D7 specifically would reproduce similar phenotypes as pan-PDE4D knockdown in VECs under FSS in reducing expression of *KLF2*, *eNOS* and *TM*. In primary VECs exposed to low or high FSS, knockdown of PDE4D7 significantly reduced the expression of each of *KLF2*, *eNOS* and *TM*. These findings are consistent with the idea that PDE4D7 regulates VEC transcriptional responses to FSS. The degree of reduction of each of *KLF2*, *eNOS* and *TM* were not identical to those seen with the pan-PDE4D knockdown, but on the same order of magnitude. Differences in siRNA efficiency, or off-target effects of other PDE4D splice variants, may account for these modest differences. Interestingly, similar PDE4D7-mediated effects were observed in the teloHAECs after 20 dyne/cm^2 of FSS, despite their inability to replicate pan-PDE4D-mediated phenotypes. These data only reinforce the importance of PDE4D7 in the context of controlling VEC transcriptional responses to FSS.

5.4 Knockdown of PDE4D5 does not impair adaptive response to FSS

With the role of PDE4D7 in VEC adaptive response to FSS identified, we turned our attention to PDE4D5. It was unknown whether PDE4D7 exerts these effects on its own, or whether it is shared by PDE4D5, with which it shares 87% of its amino acid sequence. We expected that PDE4D7 was acting alone in to transduce adaptive FSS signals. VECs treated with siRNA for PDE4D5 and exposed to low or high FSS did not have any significant differences in the expression of *KLF2*, *eNOS* or *TM*. Even with knockdown efficiency as good or better than any siRNA used in this study (~80% reduction in mRNA expression), PDE4D5 did not produce any measurable changes. These data suggest that PDE4D5 does not have a role in VEC adaptive responses to FSS, especially given the lack of effect on master flow-responsive transcription factor *KLF2*. This finding is of particular interest given a previous paper[82] detailing the role of PDE4D5 binding to integrin α5 to modulate matrix-dependent FSS signals. The authors found that PDE4D5 regulated the expression of NF-κB-induced adhesion markers on VECs exposed to oscillatory FSS. It is possible that different PDE4D splice variants might have different FSS-transducing roles dependent on context and flow type. The authors of the aforementioned study described the interactions and downstream effects they observed as being dependent on extracellular matrix, something the group had observed previously[40]. Specifically, the integrin α5β1 was activated only on fibronectin and not collagen. Presently, our FSS-related experiments were all performed on slides coated with fibronectin, and not any other extracellular matrix material. Although we would expect that any PDE4D5-mediated effects should therefore be observable on fibronectin ECM, this raises questions of matrix-specific signalling for PDE4D7 as well. It may also act in a manner dependent on the composition of the underlying ECM, something that could be investigated further in the future.

5.5 Adhesion molecule expression is minimally impacted by PDE4D5/7

Several studies have examined the relationship between FSS and VEC expression of adhesion molecules ICAM-1 and VCAM-1[25,63]. The expression of these proteins is mediated by NF-κB, which evidence suggests may itself be regulated by PDE4D5[82]. It was therefore relevant to extend our panel of FSS-responsive transcripts to assess the expression of ICAM-1, VCAM-1, as well as the inhibitory subunit of NF-κB, IκB-α. Transactivation potential of NF-κB can be measured accurately by RT-qPCR through IκB-α transcript expression[93]. Surprisingly, we found little effect of either PDE4D5 or PDE4D7 knockdowns on the expression of these inflammatory mediators. Under low laminar (3 dyne/cm^2) conditions, PDE4D5 knockdown modestly increased the expression of IκB-α. Notably, under high laminar (20 dyne/cm^2) FSS, both PDE4D5/7 knockdowns significantly reduced the expression of VCAM-1. Based on the clear impact of PDE4D7 on adaptive gene expression, its lack of influence on inflammatory gene expression was surprising. As well, based on previous reports[82], we expected PDE4D5 to have some bearing on ICAM-1 and IκB-α levels, given its importance in regulating these under oscillatory FSS. However, these data are suggestive of possible roles for both these splice variants acting in certain situations (ie. FSS levels) and only on specific genes. The lack of all-encompassing effects strengthens the idea that targeting a particular PDE4D splice variant pharmacologically could enhance desired specificity, with fewer off-target effects.

5.6 Implications for atherosclerosis

This work has revealed considerations for therapeutic targets for atherosclerosis. Reducing VEC dysfunction and increasing atheroprotective, anti-inflammatory phenotypic properties of VECs could be an effective strategy to prevent or treat atherosclerosis. Given that atherosclerotic plaques form preferentially in regions of disturbed / low FSS, targeting therapies to cells in those locations would be the most effective. Based on our findings that PDE4D7 is an important regulator allowing VECs to behave adaptively in situations of both low and high FSS, activating PDE4D7 pharmacologically could allow VECs to sense FSS more readily and change their phenotype accordingly. Pharmacological agents that stabilize the interactions between PDE4D7, EPAC1 and VE-cadherin might also have this effect. Currently, activators of PDE4s that are selective for either short-form or long-form splice variants are being developed. Based on our findings, small molecules of this type targeting long-form PDE4D variants might be particularly useful for the treatment or prevention of atherosclerosis. Pan-PDE4 targeted small molecule inhibitors are limited by severe emetic effects[9], so increasing specificity when designing drugs for PDE4 isoforms is critical. Therapies that seek to improve VEC function may be useful either as a preventative strategy for populations at sick of atherosclerosis, or as a treatment for those already afflicted by it. Improving VEC functions may slow atherogenic progression, and reduce the likelihood of critical stenosis or plaque rupture.

5.7 Limitations

There are limitations to the experimental protocols used that merit discussion. One such limitation is that the FSS applied during our experiments was constant, and not necessarily representative of FSS found in large arteries. Normally, except in patients with a mechanical pumping ventricular assist device installed, the flow in arteries is pulsatile with the heart rate. The magnitude of FSS changes with each beat, rather than remaining at a constant level. Although this does have important implications, the responses of VECs in culture to constant vs. pulsatile flow are very similar. In fact, the expression of *KLF2*, *eNOS* and *TM* in VECs under constant FSS (18 dyne/cm^2) are only slightly elevated compared to VECs under pulsatile FSS (18 dyne/cm^2 ±9 dyne/cm^2, 1 Hz)[94]. We are therefore comfortable with using constant FSS rather than pulsatile FSS as a model in our studies, however, exploring different profiles and types of FSS remains relevant to future work and important to note when contextualizing these findings.

Another limitation is that the primary HAECs used were derived from explants from a limited number of donors, and not pooled samples. This is particularly important to note given that certain results, such as PDE4D and EPAC1 knockdowns impairing adaptive responses to FSS, were only observed in these cells and not in the teloHAECs. Reproducing these experiments in arterial VECs mixed donor pools, would perhaps be more generalizable. Nevertheless, the observation of PDE4D7-mediated effects in both primary and immortalized HAECs suggests this is the case.

To assess VEC adaptive responses, mRNA transcript levels were measured by RT-qPCR. Although this is valuable data, it is not always indicative of the relative abundances of the translated proteins in cells. Measurement of protein levels, either by western blot or immunohistochemistry, would be more comprehensive. Studies have established correlations between mRNA and protein levels, but that RNA-to-protein ratios differ for each gene[95]. In our experiments, we wished to assess the expression of a panel of genes simultaneously, making mRNA measurement by RT-qPCR a practical choice. Future studies could confirm changes in protein levels.

It is also necessary to also mention limitations to potential outcomes of this work. Firstly, PDE4D7 expression is by no means confined to VECs. For instance, our lab has ongoing research into the effects of PDE4D7 on VSMC migration and tail retraction. Perhaps PDE4D7-targeted therapies might have synergistic vaso-protective effects on VECs and VSMCs, but they might also have undesired effects on blood vessels or other tissues. PDE4D7 expression is downregulated in androgen-independent prostate cancer cells, but upregulated in other prostate cancer cells but in tumours with the worst prognosis[96,97]. Although the exact role of PDE4D7 is unclear, whether it is expressed either as a pro-cancerous agent or as compensatory response to more metastatic tumours, possible involvement in these processes cautions that targeting it with activators or inhibitors might have undesired effects. Despite these concerns, targeting one splice variant rather than all PDE4(D) would likely afford benefits in the form of reduced off-target effects.

5.8 Future Directions

There are still several questions left unanswered with regards to the comprehensive roles of PDE4D7 in regulating VEC function, as well as how the overall importance of the signalling complex in cardiovascular disease.

5.8.1 Additional metrics potentially mediated by PDE4D7

Future studies may want to consider assessing additional metrics mediated by PDE4D7. These include barrier function, leukocyte adhesion and transmigration. We showed that PDE4D7 exerts effects on morphology as well as *KLF2*, *eNOS* and *TM* expression, but there are more components to a well-rounded FSS response. These would be relevant to explore at in the context of flow and atherogenesis. Furthermore, recent development of precise tools to study cAMP signalling could allow for an even closer look at the signalling functions. The use of recently generated Forester resonance energy transfer (FRET) sensors enables the study of protein-protein interactions as well as cAMP signalling in living cells. These could be utilized to explore FSS-mediated signalling and functions of PDE4D7 in real-time with fluorescence microscopy. Our lab has generated teloHAEC-based FRET probe expressing cell lines, which may or may not be useful based on the limitations of those cells herein described.

5.8.2 Matrix-dependent FSS responses

Another future direction would be to assess the matrix-dependency required for signalling events by EPAC1 and PDE4D7 in response to FSS. We have used fibronectin, but in preliminary studies have observed morphological differences with EPAC1 knockdown cells on collagen. It is likely, based on previous matrix-focused studies[40], that VEC responses and functions of particular signalling complexes differ dependent on the composition of the subcellular ECM.

Future studies could further explore these relationships by testing roles of PDE4D7 on fibronectin compared to collagen type I and IV, laminin, and others. The composition of ECM in arteries is a dynamic mix of these proteins, and changes based on environment and cell phenotype. It is therefore pertinent to investigate how each impacts VEC signalling.

5.8.3 Cell line-based investigation of PDE4D7

Ideally, teloHAECs would have been a suitable model for study of PDE4D(7) signalling. In the scenario that a novel immortalized VEC line is validated for such studies, there are numerous ways to further explore PDE4D7's signalling roles. Our initial plans called for the transfection and selection of cells expressing PDE4D7 with point mutation D559A, rendering it catalytically inactive. This approach with this construct has been used previously[97], and could elucidate the extent to which PDE4D7 is functioning as a tether for EPAC1 and VE-cadherin, as an enzyme catalyzing the hydrolysis of cAMP, or both. Future studies could compare the FSS responses of VECs stably expressing either catalytically inactive PDE4D7 or wild-type PDE4D7, in addition to other mutants such as S42A (PDE4D7 unable to be phosphorylated by PKA) or the N-terminal fragment of PDE4D7 alone. Furthermore, CRISPR-Cas9 editing approaches can be used to delete or modify regions of PDE4D7 or EPAC1 to investigate their effects on VEC FSS signaling. All these approaches require the use of a suitable immortalized VEC line, and currently teloHAECs may not be appropriate.

5.8.4 Animal models of PDE4D7

Another useful study to conduct, and a logical next step for this research, would be to move to an animal model of atherosclerosis to investigate the impacts of PDE4D7 signalling. For example, a mouse knockout model of PDE4D7, included in an ApoE -/- mouse model of atherosclerosis, could determine whether PDE4D7 signalling influences the development of atherosclerotic plaques in arteries of animals. Based on current results, one could hypothesize that a PDE4D7-knockout mouse model of atherosclerosis would have large plaque area, faster lesion development, and increased mortality due to increased VEC dysfunction resulting from lower *KLF2*, *eNOS* and *TM* expression. Another model to consider would be zebrafish, which have several advantages such as live imaging tools, express PDE4D, and can also be used as a model for atheroma formation[98]. To truly consider PDE4D7 as a potential therapeutic target for atherosclerosis, studies must be carried out at some point in animal models of the disease.

Bibliography

1. Shaaban, A. M. & Duerinckx, A. J. Wall shear stress and early atherosclerosis: a review. *AJR Am J Roentgenol* **174,** 1657–1665 (2000).
2. Conway, D. E., Williams, M. R., Eskin, S. G. & McIntire, L. V. Endothelial cell responses to atheroprone flow are driven by two separate flow components: low time-average shear stress and fluid flow reversal. *American Journal of Physiology - Heart and Circulatory Physiology* **298,** H367–74 (2010).
3. Davies, P. F. Hemodynamic shear stress and the endothelium in cardiovascular pathophysiology. *Nature Clinical Practice Cardiovascular Medicine* **6,** 16–26 (2009).
4. White, S. J. *et al.* Characterization of the differential response of endothelial cells exposed to normal and elevated laminar shear stress. *Journal of Cellular Physiology* **226,** 2841–2848 (2011).
5. Komarova, Y. A., Kruse, K., Mehta, D. & Malik, A. B. Protein Interactions at Endothelial Junctions and Signaling Mechanisms Regulating Endothelial Permeability. *Circ. Res.* **120,** 179–206 (2017).
6. Rampersad, S. N. *et al.* Cyclic AMP phosphodiesterase 4D (PDE4D) Tethers EPAC1 in a vascular endothelial cadherin (VE-Cad)-based signaling complex and controls cAMP-mediated vascular permeability. *J. Biol. Chem.* **285,** 33614–33622 (2010).
7. Rampersad, S. N. *et al.* EPAC1 promotes adaptive responses in human arterial endothelial cells subjected to low levels of laminar fluid shear stress: Implications in flow-related endothelial dysfunction. *Cellular Signalling* **28,** 606–619 (2016).
8. Rampersad, S. N., Wudwud, A., Hubert, F. & Maurice, D. H. Adaptive phenotypic modulation of human arterial endothelial cells to fluid shear stress-encoded signals: modulation by phosphodiesterase 4D-VE-cadherin signalling. *Cellular Signalling* **28,** 741–748 (2016).
9. Maurice, D. H. *et al.* Advances in targeting cyclic nucleotide phosphodiesterases. *Nat Rev Drug Discov* **13,** 290–314 (2014).
10. Monahan-Earley, R., Dvorak, A. M. & Aird, W. C. Evolutionary origins of the blood vascular system and endothelium. *Journal of Thrombosis and Haemostasis* **11,** 46–66 (2013).
11. Mulligan-Kehoe, M. & Simons, M. Vasa Vasorum in Normal and Diseased Arteries. *Circulation* **129,** (2014).
12. Majesky, M. W., Dong, X. R., Hoglund, V., Daum, G. & Mahoney, W. M. The adventitia: a progenitor cell niche for the vessel wall. *Cells Tissues Organs (Print)* **195,** 73–81 (2012).
13. Hadjiisky, P., Peyri, N. & Grosgogeat, Y. Tunica media changes in the spontaneously hypertensive rat (SHR). *Atherosclerosis* **65,** 125–137 (1987).
14. Michiels, C. Endothelial cell functions. *Journal of Cellular Physiology* **196,** 430–443 (2003).
15. Pober, J. S. & Sessa, W. C. Evolving functions of endothelial cells in inflammation. *Nature Reviews Immunology* **7,** 803–815 (2007).
16. Civelek, M. *et al.* Prelesional arterial endothelial phenotypes in hypercholesterolemia: universal ABCA1 upregulation contrasts with region-specific gene expression in vivo. *American Journal of Physiology - Heart and Circulatory Physiology* **298,** H163–70 (2010).
17. Lucitti, J. L. *et al.* Vascular remodeling of the mouse yolk sac requires hemodynamic force. *Development* **134,** 3317–3326 (2007).
18. Rajendran, P. *et al.* The vascular endothelium and human diseases. *International Journal of Biological Sciences* **9,** 1057–1069 (2013).
19. Phinikaridou, A., Hua, N., Pham, T. & Hamilton, J. A. Regions of low endothelial shear stress colocalize with positive vascular remodeling and atherosclerotic plaque disruption an in vivo magnetic resonance imaging study. *Circulation: Cardiovascular Imaging* **6,** 302–310 (2013).

20. Odagiri, K. *et al.* Non-invasive evaluation of pulmonary arterial blood flow and wall shear stress in pulmonary arterial hypertension with 3D phase contrast magnetic resonance imaging. *SpringerPlus* **5,** 1–11 (2016).
21. Taylor, C. A. & Steinman, D. A. Image-based modeling of blood flow and vessel wall dynamics: applications, methods and future directions: Sixth International Bio-Fluid Mechanics Symposium and Workshop, March 28-30, 2008 Pasadena, California. *Ann Biomed Eng* **38,** 1188–1203 (2010).
22. Hahn, C. & Schwartz, M. A. Mechanotransduction in vascular physiology and atherogenesis. *Nature Reviews Molecular Cell Biology* **10,** 53–62 (2009).
23. Stone, P. H. *et al.* Regions of low endothelial shear stress are the sites where coronary plaque progresses and vascular remodelling occurs in humans: An in vivo serial study. *European Heart Journal* **28,** 705–710 (2007).
24. Zhao, S. *et al.* Synergistic Effects of Fluid Shear Stress and Cyclic Circumferential Stretch on Vascular Endothelial Cell Morphology and Cytoskeleton. *Arteriosclerosis, Thrombosis, and Vascular Biology* **15,** 1781–1786 (1995).
25. Passerini, A. G. *et al.* Coexisting proinflammatory and antioxidative endothelial transcription profiles in a disturbed flow region of the adult porcine aorta. *Proceedings of the National Academy of Sciences of the United States of America* **101,** 2482–2487 (2004).
26. Ku, D. N., Giddens, D. P., Zarins, C. K. & Glagov, S. Pulsatile flow and atherosclerosis in the human carotid bifurcation. Positive correlation between plaque location and low oscillating shear stress. *Arteriosclerosis* **5,** 293–302 (1985).
27. White, C. R. & Frangos, J. A. The shear stress of it all: the cell membrane and mechanochemical transduction. *Philos. Trans. R. Soc. Lond., B, Biol. Sci.* **362,** 1459–1467 (2007).
28. Conway, D. E. *et al.* Fluid Shear Stress on Endothelial Cells Modulates Mechanical Tension across VE-Cadherin and PECAM-1. *Current Biology* **23,** 1024–1030 (2013).
29. Picart, C., Piau, J.-M., Galliard, H. & Carpentier, P. Human blood shear yield stress and its hematocrit dependence. *Journal of Rheology* **42,** 1–12 (1998).
30. Chachisvilis, M., Zhang, Y.-L. & Frangos, J. A. G protein-coupled receptors sense fluid shear stress in endothelial cells. *Proceedings of the National Academy of Sciences of the United States of America* **103,** 15463–15468 (2006).
31. Bass, M. D. & Humphries, M. J. Cytoplasmic interactions of syndecan-4 orchestrate adhesion receptor and growth factor receptor signalling. *Biochem. J.* **368,** 1–15 (2002).
32. Florian, J. A. *et al.* Heparan sulfate proteoglycan is a mechanosensor on endothelial cells. *Circ. Res.* **93,** e136–42 (2003).
33. Ebong, E. E., Lopez-Quintero, S. V., Rizzo, V., Spray, D. C. & Tarbell, J. M. Shear-induced endothelial NOS activation and remodeling via heparan sulfate, glypican-1, and syndecan-1. *Integr Biol (Camb)* **6,** 338–347 (2014).
34. Dinsmore, C. & Reiter, J. F. Endothelial primary cilia inhibit atherosclerosis. *EMBO Rep.* **17,** 156–166 (2016).
35. Kwon, R. Y., Temiyasathit, S., Tummala, P., Quah, C. C. & Jacobs, C. R. Primary cilium-dependent mechanosensing is mediated by adenylyl cyclase 6 and cyclic AMP in bone cells. *FASEB J.* **24,** 2859–2868 (2010).
36. Dummer, A. *et al.* Endothelial dysfunction in pulmonary arterial hypertension: loss of cilia length regulation upon cytokine stimulation. *Pulmonary Circulation* **8,** 2045894018764629 (2018).
37. Bhattacharyya, S. *et al.* Cdc42 activation couples fluid shear stress to apical endocytosis in proximal tubule cells. *Physiol Rep* **5,** e13460 (2017).

38. Tzima, E., del Pozo, M. A., Shattil, S. J., Chien, S. & Schwartz, M. A. Activation of integrins in endothelial cells by fluid shear stress mediates Rho-dependent cytoskeletal alignment. *The EMBO Journal* **20,** 4639–4647 (2001).
39. Nakajima, H. & Mochizuki, N. Flow pattern-dependent endothelial cell responses through transcriptional regulation. *Cell Cycle* **16,** 1893–1901 (2017).
40. Orr, A. W., Ginsberg, M. H., Shattil, S. J., Deckmyn, H. & Schwartz, M. A. Matrix-specific suppression of integrin activation in shear stress signaling. *Mol Biol Cell* **17,** 4686–4697 (2006).
41. Orr, A. W. *et al.* Matrix-specific p21-activated kinase activation regulates vascular permeability in atherogenesis. *J. Cell Biol.* **176,** 719–727 (2007).
42. Chachisvilis, M., Zhang, Y.-L. & Frangos, J. A. G protein-coupled receptors sense fluid shear stress in endothelial cells. *Proceedings of the National Academy of Sciences* **103,** 15463–15468 (2006).
43. Xu, J. *et al.* GPR68 Senses Flow and Is Essential for Vascular Physiology. *Cell* **173,** 762–775.e16 (2018).
44. Wiley, S. Z. *et al.* GPR68, a proton-sensing GPCR, mediates interaction of cancer-associated fibroblasts and cancer cells. *FASEB J.* **32,** 1170–1183 (2018).
45. Tzima, E. *et al.* A mechanosensory complex that mediates the endothelial cell response to fluid shear stress. *Nature* **437,** 426–431 (2005).
46. Conway, D. E. & Schwartz, M. A. Mechanotransduction of shear stress occurs through changes in VE-cadherin and PECAM-1 tension: implications for cell migration. *Cell Adh Migr* **9,** 335–339 (2015).
47. Chiu, Y.-J., McBeath, E. & Fujiwara, K. Mechanotransduction in an extracted cell model: Fyn drives stretch- and flow-elicited PECAM-1 phosphorylation. *J. Cell Biol.* **182,** 753–763 (2008).
48. Davies, P. F. Flow-mediated endothelial mechanotransduction. *Physiol. Rev.* **75,** 519–560 (1995).
49. Lagendijk, A. K. *et al.* Live imaging molecular changes in junctional tension upon VE-cadherin in zebrafish. *Nature Communications* **8,** 1402 (2017).
50. Morini, M. F. *et al.* VE-Cadherin-Mediated Epigenetic Regulation of Endothelial Gene Expression. *Circ. Res.* **122,** 231–245 (2018).
51. Zhou, J., Li, Y.-S. & Chien, S. Shear stress-initiated signaling and its regulation of endothelial function. *Arteriosclerosis, Thrombosis, and Vascular Biology* **34,** 2191–2198 (2014).
52. Chen, B. P. *et al.* DNA microarray analysis of gene expression in endothelial cells in response to 24-h shear stress. *Physiological Genomics* **7,** 55–63 (2001).
53. Davies, P. F., Civelek, M., Fang, Y. & Fleming, I. The atherosusceptible endothelium: endothelial phenotypes in complex haemodynamic shear stress regions in vivo. *Cardiovascular Research* **99,** 315–327 (2013).
54. Andersson, M. *et al.* Differential global gene expression response patterns of human endothelium exposed to shear stress and intraluminal pressure. *J. Vasc. Res.* **42,** 441–452 (2005).
55. Dekker, R. J. *et al.* Prolonged fluid shear stress induces a distinct set of endothelial cell genes, most specifically lung Krüppel-like factor (KLF2). *Blood* **100,** 1689–1698 (2002).
56. Baeyens, N., Bandyopadhyay, C., Coon, B. G., Yun, S. & Schwartz, M. A. Endothelial fluid shear stress sensing in vascular health and disease. *J. Clin. Invest.* **126,** 821–828 (2016).
57. Dai, G. *et al.* Biomechanical forces in atherosclerosis-resistant vascular regions regulate endothelial redox balance via phosphoinositol 3-kinase/Akt-dependent activation of Nrf2. *Circ. Res.* **101,** 723–733 (2007).

58. Zakkar, M. *et al.* Activation of Nrf2 in endothelial cells protects arteries from exhibiting a proinflammatory state. *Arteriosclerosis, Thrombosis, and Vascular Biology* **29,** 1851–1857 (2009).
59. SenBanerjee, S. *et al.* KLF2 Is a novel transcriptional regulator of endothelial proinflammatory activation. *J. Exp. Med.* **199,** 1305–1315 (2004).
60. Villalobo, A. Nitric oxide and cell proliferation. *FEBS Journal* **273,** 2329–2344 (2006).
61. Boon, R. A. & Horrevoets, A. J. G. Key transcriptional regulators of the vasoprotective effects of shear stress. *Hamostaseologie* **29,** 39–40– 41–3 (2009).
62. Collins, T. *et al.* Transcriptional regulation of endothelial cell adhesion molecules: NF-kappa B and cytokine-inducible enhancers. *FASEB J.* **9,** 899–909 (1995).
63. Mohan, S., Mohan, N. & Sprague, E. A. Differential activation of NF-kappa B in human aortic endothelial cells conditioned to specific flow environments. *Am. J. Physiol., Cell Physiol.* **273,** C572–C578 (1997).
64. Bhullar, I. S. *et al.* Fluid shear stress activation of IkappaB kinase is integrin-dependent. *J. Biol. Chem.* **273,** 30544–30549 (1998).
65. Orr, A. W. *et al.* The subendothelial extracellular matrix modulates NF-kappaB activation by flow: a potential role in atherosclerosis. *J. Cell Biol.* **169,** 191–202 (2005).
66. Kumar, A., Lin, Z., SenBanerjee, S. & Jain, M. K. Tumor necrosis factor alpha-mediated reduction of KLF2 is due to inhibition of MEF2 by NF-kappaB and histone deacetylases. *Mol. Cell. Biol.* **25,** 5893–5903 (2005).
67. Campbell, W. B. & Falck, J. R. Arachidonic acid metabolites as endothelium-derived hyperpolarizing factors. *Hypertension* **49,** 590–596 (2007).
68. Nikmanesh, M., Shi, Z.-D. & Tarbell, J. M. Heparan sulfate proteoglycan mediates shear stress-induced endothelial gene expression in mouse embryonic stem cell-derived endothelial cells. *Biotechnol Bioeng* **109,** 583–594 (2012).
69. Lin, K. *et al.* Molecular mechanism of endothelial growth arrest by laminar shear stress. *Proceedings of the National Academy of Sciences of the United States of America* **97,** 9385–9389 (2000).
70. RALL, T. W. & SUTHERLAND, E. W. Formation of a cyclic adenine ribonucleotide by tissue particles. *J. Biol. Chem.* **232,** 1065–1076 (1958).
71. BUTCHER, R. W. & SUTHERLAND, E. W. Adenosine 3',5'-phosphate in biological materials. I. Purification and properties of cyclic 3',5'-nucleotide phosphodiesterase and use of this enzyme to characterize adenosine 3‘,5’-phosphate in human urine. *J. Biol. Chem.* **237,** 1244–1250 (1962).
72. Diaz, M. F. *et al.* Biomechanical forces promote blood development through prostaglandin E2 and the cAMP-PKA signaling axis. *J. Exp. Med.* **212,** 665–680 (2015).
73. Smith, T. K. *et al.* Bves directly interacts with GEFT, and controls cell shape and movement through regulation of Rac1/Cdc42 activity. *Proceedings of the National Academy of Sciences of the United States of America* **105,** 8298–8303 (2008).
74. Fesenko, E. E., Kolesnikov, S. S. & Lyubarsky, A. L. Induction by cyclic GMP of cationic conductance in plasma membrane of retinal rod outer segment. *Nature* **313,** 310–313 (1985).
75. Cheng, K.-T., Chan, F. L., Huang, Y., Chan, W.-Y. & Yao, X. Expression of olfactory-type cyclic nucleotide-gated channel (CNGA2) in vascular tissues. *Histochem. Cell Biol.* **120,** 475–481 (2003).
76. Bader, A. *et al.* Adenosine receptors regulate gap junction coupling of the human cerebral microvascular endothelial cells hCMEC/D3 by Ca2+ influx through cyclic nucleotide-gated channels. *J. Physiol. (Lond.)* **595,** 2497–2517 (2017).
77. Houslay, M. D., Baillie, G. S. & Maurice, D. H. cAMP-Specific phosphodiesterase-4 enzymes in the cardiovascular system: a molecular toolbox for generating compartmentalized cAMP signaling. *Circ. Res.* **100,** 950–966 (2007).

78. Richter, W., Jin, S.-L. C. & Conti, M. Splice variants of the cyclic nucleotide phosphodiesterase PDE4D are differentially expressed and regulated in rat tissue. *Biochem. J.* **388,** 803–811 (2005).
79. Sun, Y. *et al.* Association between the PDE4D gene and ischaemic stroke in the Chinese Han population. *Clin. Sci.* **117,** 265–272 (2009).
80. Song, Y.-L. *et al.* Phosphodiesterase 4D polymorphisms associate with the short-term outcome in ischemic stroke. *Nature Publishing Group* **7,** 42914 (2017).
81. Parikh, N. & Chakraborti, A. K. Phosphodiesterase 4 (PDE4) Inhibitors in the Treatment of COPD: Promising Drug Candidates and Future Directions. *Curr. Med. Chem.* **23,** 129–141 (2016).
82. Yun, S. *et al.* Interaction between integrin α5 and PDE4D regulates endothelial inflammatory signalling. *Nature Cell Biology* **18,** 1043–1053 (2016).
83. Meyer, C. J. *et al.* Mechanical control of cyclic AMP signalling and gene transcription through integrins. *Nature Cell Biology* **2,** 666–668 (2000).
84. Lecarpentier, E. *et al.* Fluid Shear Stress Promotes Placental Growth Factor Upregulation in Human Syncytiotrophoblast Through the cAMP-PKA Signaling Pathway. *Hypertension* **68,** 1438–1446 (2016).
85. Malek, A. M., Greene, A. L. & Izumo, S. Regulation of endothelin 1 gene by fluid shear stress is transcriptionally mediated and independent of protein kinase C and cAMP. *Proceedings of the National Academy of Sciences of the United States of America* **90,** 5999–6003 (1993).
86. Fukuhara, S. *et al.* Cyclic AMP potentiates vascular endothelial cadherin-mediated cell-cell contact to enhance endothelial barrier function through an Epac-Rap1 signaling pathway. *Mol. Cell. Biol.* **25,** 136–146 (2005).
87. ATCC. ***TeloHAEC (ATCC CRL-4052)***
.
88. Yuan, L. *et al.* A role of stochastic phenotype switching in generating mosaic endothelial cell heterogeneity. *Nature Communications* **7,** 10160 (2016).
89. Zhang, Y., Toh, L., Lau, P. & Wang, X. Human telomerase reverse transcriptase (hTERT) is a novel target of the Wnt/β-catenin pathway in human cancer. *J. Biol. Chem.* **287,** 32494–32511 (2012).
90. Takano, H., Murasawa, S. & Asahara, T. Functional and gene expression analysis of hTERT overexpressed endothelial cells. *Biologics* **2,** 547–554 (2008).
91. Liu, H. *et al.* hTERT promotes cell adhesion and migration independent of telomerase activity. *Nature Publishing Group* **6,** 22886 (2016).
92. Indran, I. R., Hande, M. P. & Pervaiz, S. hTERT overexpression alleviates intracellular ROS production, improves mitochondrial function, and inhibits ROS-mediated apoptosis in cancer cells. *Cancer Res.* **71,** 266–276 (2011).
93. Bottero, V., Imbert, V., Frelin, C., Formento, J.-L. & Peyron, J.-F. Monitoring NF-kappa B transactivation potential via real-time PCR quantification of I kappa B-alpha gene expression. *Mol. Diagn.* **7,** 187–194 (2003).
94. Rossi, J. *et al.* Differential response of endothelial cells to simvastatin when conditioned with steady, non-reversing pulsatile or oscillating shear stress. *Ann Biomed Eng* **39,** 402–413 (2011).
95. Edfors, F. *et al.* Gene-specific correlation of RNA and protein levels in human cells and tissues. *Mol. Syst. Biol.* **12,** 883 (2016).
96. Böttcher, R. *et al.* Human phosphodiesterase 4D7 (PDE4D7) expression is increased in TMPRSS2-ERG-positive primary prostate cancer and independently adds to a reduced risk of post-surgical disease progression. *British Journal of Cancer* **113,** 1502–1511 (2015).
97. Henderson, D. J. P. *et al.* The cAMP phosphodiesterase-4D7 (PDE4D7) is downregulated in androgen-independent prostate cancer cells and mediates proliferation by compartmentalising

cAMP at the plasma membrane of VCaP prostate cancer cells. *British Journal of Cancer* **110,** 1278–1287 (2014).
98. Schlegel, A. Zebrafish Models for Dyslipidemia and Atherosclerosis Research. *Front Endocrinol (Lausanne)* **7,** 159 (2016).